NASA TECHNICAL NOTE

NASA TN D-7995

NASA TN D-7995

DEVELOPMENT AND APPLICATIONS OF TWO COMPUTATIONAL PROCEDURES FOR DETERMINING THE VIBRATION MODES OF STRUCTURAL SYSTEMS

Raymond G. Kvaternik

Langley Research Center
Hampton, Va. 23665

NATIONAL AERONAUTICS AND SPACE ADMINISTRATION • WASHINGTON, D. C. • NOVEMBER 1975

1. Report No. NASA TN D-7995	2. Government Accession No.	3. Recipient's Catalog No.
4. Title and Subtitle DEVELOPMENT AND APPLICATIONS OF TWO COMPUTATIONAL PROCEDURES FOR DETERMINING THE VIBRATION MODES OF STRUCTURAL SYSTEMS		5. Report Date November 1975
		6. Performing Organization Code
7. Author(s) Raymond G. Kvaternik		8. Performing Organization Report No. L-10279
		10. Work Unit No. 505-10-26-01
9. Performing Organization Name and Address NASA Langley Research Center Hampton, Va. 23665		11. Contract or Grant No.
		13. Type of Report and Period Covered Technical Note
12. Sponsoring Agency Name and Address National Aeronautics and Space Administration Washington, D.C. 20546		14. Sponsoring Agency Code

15. Supplementary Notes The information presented herein is based on a portion of a thesis entitled "Studies in Tilt-Rotor VTOL Aircraft Aeroelasticity" which was submitted to Case Western Reserve University, Cleveland, Ohio, in partial fulfillment of the requirements for the degree of Doctor of Philosophy in Engineering Mechanics, June 1973. Some additional material not contained in the original work is included.

16. Abstract

Two computational procedures for analyzing complex structural systems for their natural modes and frequencies of vibration are presented. Both procedures are based on a substructures methodology and both employ the finite-element stiffness method to model the constituent substructures. The first procedure is a direct method based on solving the eigenvalue problem associated with a finite-element representation of the complete structure. The second procedure is a component-mode synthesis scheme in which the vibration modes of the complete structure are synthesized from modes of substructures into which the structure is divided. The latter method provides for a significant reduction in the number of degrees of freedom through the expedient of partial modal synthesis wherein only a truncated set of the modes corresponding to each substructure is employed in the synthesizing procedure. The analytical basis of the methods contains a combination of features which enhance the generality of the procedures. The computational procedures so established are thought to be new and to exhibit a unique utilitarian character with respect to their versatility, computational convenience, and ease of computer implementation.

The computational procedures have been implemented in two special-purpose computer programs designated SUDAN and SCORE. The results of the application of these programs to several structural configurations are shown and comparisons are made with experiment. These studies, as well as others, have verified the analytical basis of the procedures and have demonstrated a wide range of engineering applicability for the SUDAN and SCORE programs.

17. Key Words (Suggested by Author(s)) Structural dynamics; Vibration analyses; Modal synthesis	18. Distribution Statement Unclassified – Unlimited. Subject Category 39

19. Security Classif. (of this report)	20. Security Classif. (of this page)	21. No. of Pages	22. Price*
Unclassified	Unclassified	65	$4.25

*For sale by the National Technical Information Service, Springfield, Virginia 22161

CONTENTS

DEVELOPMENT AND APPLICATIONS OF TWO COMPUTATIONAL PROCEDURES FOR DETERMINING THE VIBRATION MODES OF STRUCTURAL SYSTEMS*

Raymond G. Kvaternik
Langley Research Center

SUMMARY

Two computational procedures for analyzing complex structural systems for their natural modes and frequencies of vibration are presented. Both procedures are based on a substructures methodology and both employ the finite-element stiffness method to model the constituent substructures. The first procedure is a direct method based on solving the eigenvalue problem associated with a finite-element representation of the complete structure. The second procedure is a component-mode synthesis scheme in which the vibration modes of the complete structure are synthesized from modes of substructures into which the structure is divided. The latter method provides for a significant reduction in the number of degrees of freedom through the expedient of partial modal synthesis wherein only a truncated set of the modes corresponding to each substructure is employed in the synthesizing procedure. The analytical basis of the methods contains a combination of features which enhance the generality of the procedures. The computational procedures so established are thought to be new and to exhibit a unique utilitarian character with respect to their versatility, computational convenience, and ease of computer implementation.

The computational procedures have been implemented in two special-purpose computer programs designated SUDAN and SCORE. The results of the application of these programs to several structural configurations are shown and comparisons are made with experiment. These studies, as well as others, have verified the analytical basis of the procedures and have demonstrated a wide range of engineering applicability for the SUDAN and SCORE programs.

---

*The information presented herein is based on a portion of a thesis entitled "Studies in Tilt-Rotor VTOL Aircraft Aeroelasticity" which was submitted to Case Western Reserve University, Cleveland, Ohio, in partial fulfillment of the requirements for the degree of Doctor of Philosophy in Engineering Mechanics, June 1973. Some additional material not contained in the original work is included.

INTRODUCTION

A fundamental problem in the design of aerospace vehicle structures is the determination of the natural modes and frequencies of vibration. These data constitute the essential ingredient in aeroelastic stability and response analyses which employ the normal mode method to establish the system equations of motion. Two basic approaches for analyzing aerospace structures for their natural modes and frequencies of vibration have been established in the literature. The first approach is a direct method based on constructing a finite-element model of the structure and solving the resulting matrix eigenvalue problem for the system modes and frequencies (refs. 1 to 7). For large structures, such as those exemplified by the space shuttle, the number of degrees of freedom associated with such an approach may be excessive, resulting in prohibitive execution times and large computer central-memory requirements. The second approach is component-mode synthesis (refs. 8 to 23) which is based on the concept of employing the modes of conveniently defined components, or substructures, into which the structure is divided in order to synthesize the modes of the complete structure. The expedient of reducing the number of system degrees of freedom, and thus the size of the computing task is introduced by using only a truncated set of the modes corresponding to each component in the synthesizing procedure. The latter method is thus uniquely suited to the analysis of structures which are too large to be treated by the direct method.

Two general computational procedures for calculating the natural vibratory modes and frequencies of structural systems are presented. One is a direct method and the other is a component-mode synthesis scheme. Both procedures are based on a substructures methodology and employ the finite-element stiffness method to model the constituent substructures. Salient features common to both the direct and component-mode synthesis procedures include: the imposition of the compatibility relations on the substructure attachment coordinates according to an algorithm conceived by Walton and Steeves (ref. 24); the assumption of a full (i.e., nondiagonal) mass matrix; and the ability to treat the case in which both the mass and stiffness matrices are singular simultaneously, in contrast to the usual assumption that one or the other is nonsingular. Additional features are incorporated in the component-mode synthesis formulation. A hybrid coordinate representation whereby both modal and discrete coordinates can be employed simultaneously is included. The component-mode shapes used are completely arbitrary with respect to their origin, type, and normalization in that the mode shapes can be either for free or restrained support conditions; can consist of either calculated or measured modes, static deflection shapes, assumed deflection shapes, or any combination of these; and need not be orthogonal or normalized in any consistent manner. A unified treatment of the component-mode shapes is employed in the synthesizing procedure, without recourse to matrix partitioning according to the type of component modes employed. The combination of these features in the direct and component-mode synthesis formulations described herein is thought to be new and to provide the basis for computational procedures which are unique with respect to their generality, computational convenience, and ease of computer implementation.

The computational procedures described are general and apply to a structural discretization based on any type of finite element. The procedures have been implemented in two special-purpose computer programs designated SUDAN (SUbstructuring in Direct ANalyses) and SCORE (Synthesis of COmponent REsponses). The results of the application of SUDAN and SCORE to several structural configurations are shown. These configurations include: a free-free beam; an assembly of beams configured in the shape of an airplane; a 1/15-scale dynamic model of an early space shuttle concept; and a 1/30-scale dynamic, aeroelastic model of a B-52E airplane. Comparisons are also made with experimental results for three of the configurations. These studies, as well as others for a variety of airframe dynamic analyses in support of various projects, have verified the analytical basis of these procedures and demonstrated a wide range of engineering applicability for the SUDAN and SCORE programs.

SYMBOLS

Physical quantities in this report are given in the International System of Units (SI). U.S. Customary Units, if shown, are given parenthetically. All measurements and calculations were made in U.S. Customary Units.

$[B]$	symmetric matrix constructed from the coefficients of the constraint equations
$[B_{11}]$	submatrix of $[B]$
$[C]$	matrix of coefficients of constraint equations expressed in discrete, physical coordinates
$[C_1]$, $[C_2]$	submatrices of $[C]$
$[D]$	matrix of coefficients of constraint equations expressed in modal coordinates
$[D_1]$, $[D_2]$	submatrices of $[D]$
$[E]$	symmetric matrix constructed from the coefficients of the constraint equations

EI	bending stiffness of beam
f_c	calculated frequency, Hz
f_m	measured frequency, Hz
GJ	torsional stiffness of beam
$[I]$	unit matrix
$[K]$	generalized stiffness matrix of assembled structure
$[\overline{K}]$	composite matrix containing free-body stiffness matrices of substructures as submatrices on the principal diagonal
$[\mathcal{K}]^{(i)}$	modal stiffness matrix for ith substructure
$[k]^{(i)}$	stiffness matrix of ith substructure regarded as a free body
L	Lagrangian function
$[M]$	generalized mass matrix of assembled structure
$[\overline{M}]$	composite matrix containing free-body mass matrices of substructures as submatrices on the principal diagonal
$[\mathcal{M}]^{(i)}$	modal mass matrix for ith substructure
$[m]^{(i)}$	mass matrix of ith substructure regarded as a free body
N	total number of discrete, physical coordinates describing the substructures
NS	number of substructures into which system is divided
NSM	total number of substructure modes employed in the synthesizing procedure
$\{p\}^{(i)}$	column matrix of discrete, physical coordinates for ith substructure regarded as a free body

$[Q]$	modal matrix containing eigenvectors of system mass matrix $[M]$
$\{q\}$	column matrix of generalized coordinates
$\{q_o\}$	column matrix containing amplitudes of generalized coordinates
r	number of constraint equations
$[S]$	generalized stiffness matrix; permutation matrix
$\left[S_{11}\right]$, $\left[S_{12}\right]$, $\left[S_{21}\right]$, $\left[S_{22}\right]$	submatrices of generalized stiffness matrix $[S]$
$[\hat{S}]$	generalized stiffness matrix
$[\tilde{S}]$	reduced generalized stiffness matrix
$[U]$	uncoupled system modal expansion matrix containing substructure modal subsets $[U]^{(i)}$ on principal diagonal
$[U]^{(i)}$	subset of modes for ith substructure
$[X]$	matrix of eigenvectors for constraint eigenvalue problem
$\{x\}$, $\{y\}$	column matrices
$[Y]$	composite matrix containing $\left[Y_1\right]$ and $\left[Y_2\right]$ as submatrices on principal diagonal
$\left[Y_1\right]$	matrix of eigenvectors of $\left[B_{11}\right]$
$\left[Y_2\right]$	matrix of eigenvectors of $[0]$
$\{y_1\}$, $\{y_2\}$	submatrices of $\{y\}$

$\{z\}$	column matrix containing the discrete, physical coordinates of all the substructures
$\{z_1\}$, $\{z_2\}$	submatrices of $\{z\}$
$\{z\}_i$	ith mode shape of system in discrete, physical coordinates
$[\beta]$	connectivity matrix which enforces geometric compatibility at the interfaces of the substructures
$\{\eta\}$, $\{\hat{\eta}_1\}$	column matrices of generalized coordinates
$\{\eta_1\}$, $\{\eta_2\}$	submatrices of $\{\eta\}$
$\{\hat{\eta}_1\}_i$	ith mode shape of system in generalized coordinates
λ	eigenvalue
λ_i	ith eigenvalue
$\lceil\lambda\rfloor$	diagonal matrix of eigenvalues
μ	eigenvalue
$\lceil\mu\rfloor$	diagonal matrix of eigenvalues of $[M]$
$\lceil\mu_1\rfloor$	submatrix of $\lceil\mu\rfloor$
$\{\xi\}$	column matrix containing all substructure modal coordinates
$\{\xi\}^{(i)}$	modal coordinates of ith substructure
$\{\xi_1\}$, $\{\xi_2\}$	submatrices of $\{\xi\}$

$\left[\Omega^2\right]$ diagonal matrix of squares of substructure natural frequencies

ω^2 square of natural frequency

$[0]$ null submatrix of $[B]$

Superscripts:

T denotes matrix transpose

-1 denotes matrix inverse

Primes are used to distinguish between common symbols representing matrix quantities which are different numerically.

Dots over symbols are used to denote derivatives with respect to time.

ANALYTICAL FORMULATION

Mathematical Model of Substructures

The procedures for natural mode vibration analysis by direct and component-mode synthesis techniques presented here are based on a substructures approach in which the structure is conceptually divided into separate smaller components or substructures. Such a division into substructures is schematically depicted in figure 1. The application of finite-element modeling (refs. 1 to 7) to each of the substructures regarded as a free body (i.e., with free boundary conditions) leads to a discrete mass matrix $[m]$, a discrete stiffness matrix $[k]$, and a vector of discrete coordinates[1] $\{p\}$ for each substructure. Since the substructures are treated as distinct components in a substructuring methodology, their structural properties are most conveniently defined relative to the axes local to each component. The definition of the substructure inertial and elastic matrices with respect to such local coordinate axes is assumed here. When a suitable set of substructures has been identified and the corresponding mass and stiffness matrices, $[m]^{(i)}$ and $[k]^{(i)}$, are determined, the free-vibration equation of motion for the ith substructure has the form

$$[m]^{(i)}\{\ddot{p}\}^{(i)} + [k]^{(i)}\{p\}^{(i)} = \{0\} \tag{1}$$

[1]Discrete coordinates define the translations and rotations at a set of discrete points on a structure. In contrast, distributed or modal coordinates specify the magnitude of given space distribution of displacement and thus provide information at all points on a structure (cf., ref. 4).

Collecting the equations for all the substructures into one diagonally partitioned matrix equation gives

$$\begin{bmatrix} [m]^{(1)} & & & & & \\ & [m]^{(2)} & & & & \\ & & \cdot & & & \\ & & & \cdot & & \\ & & & & \cdot & \\ & & & & & [m]^{(NS)} \end{bmatrix} \begin{Bmatrix} \{\ddot{p}\}^{(1)} \\ \{\ddot{p}\}^{(2)} \\ \cdot \\ \cdot \\ \cdot \\ \{\ddot{p}\}^{(NS)} \end{Bmatrix} + \begin{bmatrix} [k]^{(1)} & & & & & \\ & [k]^{(2)} & & & & \\ & & \cdot & & & \\ & & & \cdot & & \\ & & & & \cdot & \\ & & & & & [k]^{(NS)} \end{bmatrix} \begin{Bmatrix} \{p\}^{(1)} \\ \{p\}^{(2)} \\ \cdot \\ \cdot \\ \cdot \\ \{p\}^{(NS)} \end{Bmatrix} = \begin{Bmatrix} \{0\}^{(1)} \\ \{0\}^{(2)} \\ \cdot \\ \cdot \\ \cdot \\ \{0\}^{(NS)} \end{Bmatrix} \tag{2}$$

or, in more compact notation

$$[\overline{M}]\{\ddot{z}\} + [\overline{K}]\{z\} = \{0\} \tag{3}$$

where the diagonally partitioned form of $[\overline{M}]$ and $[\overline{K}]$ reflects the fact that the substructures are not connected.

For the substructures shown in figure 1, for example, the composite matrices $[\overline{M}]$ and $[\overline{K}]$ appearing in equation (3) would each have the form given diagrammatically in figure 2. Each block in figure 2 represents the mass or stiffness matrix appropriate to a substructure. The ordering of the substructure matrices (blocks in fig. 2) within $[\overline{M}]$ and $[\overline{K}]$ must be consistent but is otherwise arbitrary. Since the mass and stiffness matrices for each substructure are generated independently, no intersubstructure coupling exists between the partitions of $[\overline{M}]$ or $[\overline{K}]$, as indicated in figure 2.

Formulation of the Coupling Procedure and Establishing the System Equations of Motion

If the composite matrices containing the mass and stiffness matrices of the individual substructures as submatrices on the principal diagonal are denoted by $[\overline{M}]$ and $[\overline{K}]$, respectively, according to equations (2) and (3), the Lagrangian of the partitioned (i.e., uncoupled) structure can be written as

$$L = \frac{1}{2}\{\dot{z}\}^T[\overline{M}]\{\dot{z}\} - \frac{1}{2}\{z\}^T[\overline{K}]\{z\} \tag{4}$$

where $\{z\}$ is a column matrix containing the discrete, physical coordinates of all the substructures. Now a consequence of any substructuring procedure is the introduction of coordinates which are not independent but are related by equations of constraint. Such equations must be imposed to restore geometric compatibility at the interfaces. Since the matrices $[\overline{M}]$ and $[\overline{K}]$ in equation (4) have been established on the basis of such a substructuring procedure, the coordinates forming the vector $\{z\}$ are not independent.

The equations of constraint must be used to construct a transformation matrix relating the dependent coordinates $\{z\}$ to a set of independent coordinates. This transformation is then used to analytically join the individual substructure mass and stiffness matrices to arrive at the mass and stiffness matrices of the complete system.

The linear algebraic equations of constraint which follow from considerations of deflection[2] compatibility at the junctions of the substructures can be written as

$$\underset{r \times N}{[C]}\ \underset{N \times 1}{\{z\}} = \{0\} \tag{5}$$

where $[C]$ is a constant matrix depending solely on the geometric configuration of the interfaces and $\{z\}$ is the vector of discrete coordinates appearing in equation (4). In practice $[C]$ is rectangular with the number of rows r generally much less than the number of columns N. Since there are many coordinates which do not appear in the constraint equations, the matrix $[C]$ is also characterized by the presence of many null (zero) columns.

The usual practice when dealing with equations of constraint (see, for example, ref. 8) is to select certain of the coordinates as independent coordinates. The remaining (dependent) coordinates are expressed in terms of those coordinates which have been selected to be independent by solving the constraint equations as simultaneous equations. In an alternate method devised by Walton and Steeves (ref. 24),[3] the solution of the constraint equations for the independent coordinates is associated with computing the eigenvalues and eigenvectors of a symmetric matrix formed from the matrix of coefficients appearing in the constraint equations. For completeness, both methods are reviewed here.

Usual method for establishing independent coordinates.- Usual practice when dealing with equations of constraint is to partition equation (5) in the form

$$\left[\begin{array}{c:c} \underset{r \times r}{[C_1]} & \underset{r \times (N-r)}{[C_2]} \end{array}\right] \left\{\begin{array}{c} \underset{r \times 1}{\{z_1\}} \\ \\ \underset{(N-r) \times 1}{\{z_2\}} \end{array}\right\} = \{0\} \tag{6}$$

where $\{z_1\}$ is the subset of $\{z\}$ chosen to be the dependent variables and $\{z_2\}$ is the subset chosen to be the independent coordinates. The partitioning indicated in equa-

[2]Herein, deflection compatibility is used in the generic sense to include both linear and angular displacements.

[3]A modified version of their original work is also available as a National Aeronautics and Space Administration (NASA) Technical Report (ref. 25).

tion (6) is carried out by rearranging the columns of $[C]$ such that the columns of $[C_1]$ and $[C_2]$ correspond to the elements in $\{z_1\}$ and $\{z_2\}$, respectively. The selection of the independent coordinates is arbitrary except for the requirement that the choice lead to a matrix $[C_1]$ which is nonsingular. If $[C_1]$ is nonsingular, equation (6) yields

$$\{z_1\} = -[C_1]^{-1}[C_2]\{z_2\} \tag{7}$$

The vector $\{z\}$ is then related to the independent subset $\{z_2\}$ by

$$\{z\} = \left\{\begin{array}{c}\{z_1\} \\ \hdashline \{z_2\}\end{array}\right\} = \left[\begin{array}{c}-[C_1]^{-1}[C_2] \\ \hdashline [I]\end{array}\right]\{z_2\} \tag{8}$$

or, more compactly,

$$\{z\} = [\beta]\{z_2\} \tag{9}$$

Equation (9) defines a coordinate transformation from a set of constrained or dependent coordinates $\{z\}$ to a reduced set of unconstrained or independent coordinates $\{z_2\}$. The transformation matrix $[\beta]$ may be interpreted as a connectivity matrix which enforces geometric compatibility at the interfaces of the substructures. It should be noted that the independent coordinates obtained in this manner are a subset of the original dependent coordinates.

Method of Walton and Steeves for establishing independent coordinates.- In writing the constraint equations in the partitioned form given by equation (6), it has been implicitly assumed that the rank of the matrix $[C]$ is equal to the number of rows in $[C]$; that is, the equations are assumed to be linearly independent. In practice, for complex structures redundancies often inadvertently appear in the equations of constraint (ref. 26), resulting in equations which are not linearly independent. The rank of $[C]$ would then be less than the number of rows r; thus, it would not be possible to find a nonsingular partition of order $r \times r$ in $[C]$ and proceed as outlined above. Even if the rank of $[C]$ is equal to the number of rows r, in order to arrive at a nonsingular submatrix $[C_1]$ by rearranging the columns of $[C]$, it must be possible to identify the r linearly independent columns of $[C]$. This identification may not be an easy task. The method of Walton and Steeves (ref. 24) obviates the need to treat the case of redundant equations of constraint in any special manner and the necessity of being able to identify the independent columns of $[C]$. The basis of their method is a mathematical theorem designated the "zero eigenvalues theorem." This theorem expresses the solution of a set of linear homogeneous algebraic equations (such as the constraint equations) in terms of eigenvectors of a symmetric matrix constructed from the coefficients of the equations. The method proceeds as follows. With $[C]$ from equation (5) the symmetric matrix $[E]$ is constructed according to

$$[E] = [C]^T [C] \tag{10}$$

The eigenvalue problem

$$[E]\{x\} = \lambda\{x\} \tag{11}$$

is solved for all its eigenvalues and eigenvectors. The resulting set of eigenvalues can be arranged in the diagonal matrix $\left[\diagdown \lambda \diagdown\right]$ and the corresponding eigenvectors in the matrix $[X]$. Now the eigenvalues of $[E]$ are positive or zero (ref. 24). If P represents the number of eigenvalues which are zero, the most general solution of equation (5) is given by

$$\underset{N\times 1}{\{z\}} = \underset{N\times P}{[\beta]} \; \underset{P\times 1}{\{q\}} \tag{12}$$

The matrix $[\beta]$ is formed from the columns of $[X]$ which correspond to eigenvalues λ_i having the value zero, and $\{q\}$ is a column matrix of independent coordinates. If there are any redundant constraint equations, the number of positive eigenvalues resulting from the solution of the eigenvalue problem of equation (11) is equal to the number of independent equations of constraint and the matrix $[\beta]$ is still formed from the columns of $[X]$ corresponding to the zero eigenvalues of $[E]$. Equation (12) then defines a transformation from dependent coordinates $\{z\}$ to independent coordinates $\{q\}$ through the matrix $[\beta]$ which imposes the condition of geometric compatibility at the junctions of the substructures.

In summary, the problem of determining $[\beta]$ by the method of Walton and Steeves reduces to that of calculating the eigenvalues and eigenvectors of $[E]$. The independent coordinates established in this manner are not usually amenable to direct physical interpretation. However, the transformation to the original (physical) coordinates is available through equation (12). In contrast, the independent coordinates obtained by proceeding in the usual manner (discussed previously) are a subset of the original (physical), dependent coordinates.

The manner of introducing the transformation to independent coordinates and arriving at the system equations of motion is outlined here for both the direct and component-mode synthesis methods. The development is general and can accommodate a connectivity matrix $[\beta]$ arrived at in any manner. However, because of the computational conveniences associated with the method of Walton and Steeves, the adoption of their procedure is assumed here.

Substructure coupling in the direct method.- By following the procedure of reference 24 to establish $[\beta]$, a transformation to independent coordinates is effected by substituting equation (12) into the Lagrangian for the partitioned structure as given in equation (4). This substitution leads to

$$L = \frac{1}{2}\{\dot{q}\}^T[\beta]^T[\overline{M}][\beta]\{\dot{q}\} - \frac{1}{2}\{q\}^T[\beta]^T[\overline{K}][\beta]\{q\} \tag{13}$$

By defining

$$\left.\begin{aligned} [M] &\equiv [\beta]^T[\overline{M}][\beta] \\ [K] &\equiv [\beta]^T[\overline{K}][\beta] \end{aligned}\right\} \tag{14}$$

as the generalized mass and stiffness matrices of the coupled system, the Lagrangian for the assembled structure becomes

$$L = \frac{1}{2}\{\dot{q}\}^T[M]\{\dot{q}\} - \frac{1}{2}\{q\}^T[K]\{q\} \tag{15}$$

The substitution of equation (15) into Lagrange's equation for a conservative system

$$\frac{d}{dt}\left(\frac{\partial L}{\partial \dot{q}}\right) - \frac{\partial L}{\partial q} = 0 \tag{16}$$

yields

$$[M]\{\ddot{q}\} + [K]\{q\} = \{0\} \tag{17}$$

as the free-vibration equations of motion for the complete structure.

The method of Walton and Steeves requires the determination of all the eigenvalues and eigenvectors of the matrix $[E]$. Since $[E]$ is of order $N \times N$, where N is the total number of discrete coordinates describing the substructures, this eigenvalue problem constitutes a rather large computing task. Because the matrix $[E]$ is characterized by the presence of many null (zero) rows and columns, a practical computational procedure for significantly reducing the size of this eigenvalue problem and thus increasing the utility of the method of Walton and Steeves is given in the appendix.

It should be pointed out that the preceding development has explicitly considered only the case of undamped free vibration. However, the procedure can be extended to the more general case in which damping and external forces are included.

Substructure coupling in component-mode synthesis.- Component-mode synthesis is based on the concept of synthesizing the modes of the complete structure from the modes associated with the substructures into which the structure is divided. The expedient of reducing the degrees of freedom and thus the size of the system eigenvalue problem is introduced by employing a truncated set of component modes in the synthesizing procedure. The selection of the substructure modes is generally based on a frequency cutoff criterion in which only the substructure modes below the maximum frequency of interest for the complete structure are used. The substructure modes either can be computed by utilizing the discrete element analytical model available for each isolated substructure or can be obtained from ground vibration tests. Also, since the orthogonality of the component modes is not assumed, it is possible to use shape functions other than natural modes to be used alone or in conjunction with the selected subset of natural modes to describe the behavior of a component. Included in this latter category are static deflection shapes, such as the "constraint modes" of Hurty (ref. 8) and the "attachment modes" of Bamford (ref. 11), and assumed deflection shapes, such as polynomial shape functions.

In the original work of Hurty (ref. 8) the component shapes are classified into three types: rigid-body modes, constraint modes, and fixed-constraint normal modes. Rigid-body modes are associated with displacements in which no strain energy is involved. A component can have up to 6 rigid-body degrees of freedom, depending on the number of fixed external constraints. Constraint modes are the static shapes assumed by the component when each of the redundant constraints is independently given a unit displacement, all others being held fixed. As many such modes exist as there are redundant constraints in the interface connection of the component. If the connection between the substructures is statically determinate, then no constraint modes are required. Fixed-constraint normal modes are the free-vibration modes of the component with all the constraints fixed. For computational convenience Bajan and Feng (ref. 12) and Craig and Bampton (ref. 13) do not distinguish between rigid-body modes and redundant constraint modes. Their constraint modes are established by giving a unit displacement to each connection degree of freedom in turn so that no rigid-body modes occur. Any rigid-body modes associated with the component turn out to be a linear combination of the constraint modes in this case. This method works even if the constraints are statically determinate. Attachment modes are the displacements of a substructure corresponding to concentrated loads on the substructure. These were introduced by Bamford (ref. 11) to allow for the concentrated attachment forces induced by one component on another at their points of connection. The present work does not address the problem of determining the component constraint and attachment modes. These modes, when required, can be determined by straightforward static analyses utilizing the finite-element models established for the individual substructures, as described in references 12 and 22, for example. However, the present development is general and can accommodate any of these component shapes. Within the context of the present development then, any reference to substructure modes should be interpreted in the general sense to include any of these shapes.

The modes selected to define each substructure are arranged by columns in the matrices $[U]^{(i)}$. The superscript denotes the ith substructure. No restrictions are placed on the arrangement of the chosen substructure modes in $[U]^{(i)}$. The support conditions imposed for calculating or measuring the substructure modes need not correspond to the restraint conditions which exist for the substructure in the assembled configuration; in this case appropriate rigid-body modes (and possibly constraint modes and/or attachment modes) would be included in the selected set of modes. Although the modes within each subset $[U]^{(i)}$ must be linearly independent, they need not be orthogonal or normalized in any consistent manner.[4] By employing these substructure mode sets, the transformation from discrete coordinates $\{p\}^{(i)}$ to modal coordinates $\{\xi\}^{(i)}$ can be written as

$$\begin{Bmatrix} \{p\}^{(1)} \\ \{p\}^{(2)} \\ \cdot \\ \cdot \\ \cdot \\ \cdot \\ \{p\}^{(NS)} \end{Bmatrix} = \begin{bmatrix} [U]^{(1)} & & & & & & \\ & [U]^{(2)} & & & & & \\ & & \cdot & & & & \\ & & & \cdot & & & \\ & & & & \cdot & & \\ & & & & & \cdot & \\ & & & & & & [U]^{(NS)} \end{bmatrix} \begin{Bmatrix} \{\xi\}^{(1)} \\ \{\xi\}^{(2)} \\ \cdot \\ \cdot \\ \cdot \\ \cdot \\ \{\xi\}^{(NS)} \end{Bmatrix} \tag{18}$$

or, in abbreviated notation

$$\underset{N \times 1}{\{z\}} = \underset{N \times NSM}{[U]} \; \underset{NSM \times 1}{\{\xi\}} \tag{19}$$

[4]The one exception is discussed in the next section.

where NS denotes the number of substructures. The block-diagonal form of $[U]$ reflects the fact that the substructures are not connected. This fact is more clearly illustrated in figure 3 which shows the form of this matrix for the aircraft of figure 1. The number of rows in the uncoupled system modal expansion matrix $[U]$ is equal to the total number of discrete degrees of freedom for all the substructures N. The number of columns in $[U]$ is equal to the total number of selected modes NSM. The substitution of equation (19) into the Lagrangian of the partitioned structure as given by equation (4) gives

$$L = \frac{1}{2}\{\dot{\xi}\}^T[U]^T[\overline{M}][U]\{\dot{\xi}\} - \frac{1}{2}\{\xi\}^T[U]^T[\overline{K}][U]\{\xi\} \tag{20}$$

where $[\overline{M}]$ and $[\overline{K}]$ are numerically identical to the corresponding matrices in the direct method. Because of the block diagonal character of $[U]$, $[\overline{M}]$, and $[\overline{K}]$, the expanded form of the matrix products $[U]^T[\overline{M}][U]$ and $[U]^T[\overline{K}][U]$ in equation (20) can be written as

$$[U]^T[\overline{M}][U] = \begin{bmatrix} [\mathcal{M}]^{(1)} & & & & \\ & [\mathcal{M}]^{(2)} & & & \\ & & \cdot & & \\ & & & \cdot & \\ & & & & \cdot \\ & & & & & [\mathcal{M}]^{(NS)} \end{bmatrix} \tag{21a}$$

$$[U]^T[\overline{K}][U] = \begin{bmatrix} [\mathcal{K}]^{(1)} & & & & \\ & [\mathcal{K}]^{(2)} & & & \\ & & \cdot & & \\ & & & \cdot & \\ & & & & \cdot \\ & & & & & [\mathcal{K}]^{(NS)} \end{bmatrix} \tag{21b}$$

where $[\mathcal{M}]^{(i)}$ and $[\mathcal{K}]^{(i)}$ are, respectively, the modal mass and stiffness matrices for the ith substructure and are given by

$$[\mathcal{M}]^{(i)} = [U]^{(i)^T}[m]^{(i)}[U]^{(i)} \tag{22a}$$

$$[\mathcal{K}]^{(i)} = [U]^{(i)^T}[k]^{(i)}[U]^{(i)} \tag{22b}$$

If the orthogonality of the substructure modes normalized to give unit generalized mass is assumed, the matrix products $[U]^T[\overline{M}][U]$ and $[U]^T[\overline{K}][U]$ in equation (20) simplify to

$$[U]^T[\overline{M}][U] = [I] \tag{23a}$$

and

$$[U]^T[K][U] = \left\lceil \Omega^2 \right\rfloor \tag{23b}$$

The matrix $[I]$ is the unit matrix and the matrix $\left\lceil \Omega^2 \right\rfloor$ has the squares of the substructure natural frequencies corresponding to the selected modes[5] on the main diagonal. Neither the mass nor stiffness matrices of the components is explicitly required in this case. The use of free-interface component modes, such as in the synthesis schemes of Goldman (ref. 10) and Hou (ref. 14), for example, leads to the simple forms given in equations (23a) and (23b). Since in practice it is often either necessary or convenient to employ component shapes which are not orthogonal (such as attachment modes or assumed deflection shapes), the analytical procedure should be independent of the type of shapes used in the synthesizing procedure and should not require their orthonormalization to comply with equations (23a) and (23b). As already remarked, in the present formulation the orthogonality of the component modes is not assumed and utilized in forming the reduced mass and stiffness matrices in terms of modal coordinates; thereby, the use of a combination of various types of component modes corresponding to arbitrary support conditions and normalizations is permitted.

Since continuity conditions at the junctions of the substructures have not yet been imposed, the coordinates $\{\xi\}$ in equation (20) are not independent but related by equations of constraint which express kinematic dependencies among the coordinates established for the various components. These coordinates are therefore not generalized coordinates

[5]Zero frequency modes are included.

and the equations of constraint must be used to relate the dependent set $\{\xi\}$ to a reduced set of independent coordinates. The constraint equations in terms of discrete, physical coordinates are given by

$$[C]\{z\} = \{0\} \tag{24}$$

These constraint equations are identical to those which would be written if proceeding by the direct method. With the substitution of the transformation of equation (19) into equation (24), the constraint equations expressed in terms of the modal coordinates $\{\xi\}$ have the form

$$\underset{r \times N}{[C]} \; \underset{N \times NSM}{[U]} \; \underset{NSM \times 1}{\{\xi\}} = \{0\} \tag{25}$$

or

$$\underset{r \times NSM}{[D]} \; \underset{NSM \times 1}{\{\xi\}} = \{0\} \tag{26}$$

where the definition of $[D]$ follows from equation (25). The equations of constraint in the form given by equation (26) must now be used to determine a set of generalized coordinates equal in number to the total number of component modes minus the number of (independent) constraint equations.

If the usual method of dealing with equations of constraint is employed, equation (26) is partitioned in the form

$$\left[\begin{array}{c|c} \underset{r \times r}{[D_1]} & \underset{r \times (NSM-r)}{[D_2]} \end{array}\right] \left\{\begin{array}{c} \underset{r \times 1}{\{\xi_1\}} \\ \hline \underset{(NSM-r) \times r}{\{\xi_2\}} \end{array}\right\} = \{0\} \tag{27}$$

The submatrix $\{\xi_1\}$ is the subset of $\{\xi\}$ chosen to be the dependent coordinates and $\{\xi_2\}$ is the subset chosen to be the independent coordinates. When $[D_1]$ is assumed to be nonsingular, the dependency of $\{\xi_1\}$ on $\{\xi_2\}$ is given by

$$\{\xi_1\} = -[D_1]^{-1}[D_2]\{\xi_2\} \tag{28}$$

so that

$$\{\xi\} = \left\{\begin{array}{c}\{\xi_1\}\\ \hline \{\xi_2\}\end{array}\right\} = \left[\begin{array}{c}-[D_1]^{-1}[D_2]\\ \hline [I]\end{array}\right]\{\xi_2\} \tag{29}$$

or

$$\{\xi\} = [\beta']\{\xi_2\} \tag{30}$$

Again, this method requires that the rank of the matrix $[D]$ be equal to the number of rows of $[D]$ and that one be able to identify r linearly independent columns of the matrix $[D]$. Again, the method of Walton and Steeves obviates the need to treat the case of redundant equations of constraint in any special manner and the necessity of being able to identify the independent columns of $[D]$.

By following reference 24, the symmetric matrix $[E']$ is defined by

$$[E'] \equiv [D]^T[D] \tag{31}$$

The eigenvalue problem

$$[E']\{x'\} = \lambda'\{x'\} \tag{32}$$

is then solved for all its eigenvalues and eigenvectors. From the resulting matrix of eigenvectors $[X']$ those columns corresponding to eigenvalues having the value zero are selected and are used to form a matrix $[\beta']$. A suitable transformation from dependent modal coordinates $\{\xi\}$ to independent system coordinates (geometric compatibility at the interfaces of the substructures restored by the transformation) is then given by

$$\{\xi\} = [\beta']\{q'\} \tag{33}$$

The substitution of equation (33) into equation (20) gives

$$L = \frac{1}{2}\left\{\dot{q}'\right\}^T[\beta']^T[U]^T[\overline{M}][U][\beta']\left\{\dot{q}'\right\}$$

$$- \frac{1}{2}\left\{q'\right\}^T[\beta']^T[U]^T[\overline{K}][U][\beta']\left\{q'\right\} \tag{34}$$

By defining

$$\left.\begin{aligned} [M'] &\equiv [\beta']^T[U]^T[\overline{M}][U][\beta'] \\ [K'] &\equiv [\beta']^T[U]^T[\overline{K}][U][\beta'] \end{aligned}\right\} \tag{35}$$

as the generalized mass and stiffness matrices of the coupled system, equation (34) becomes

$$L = \frac{1}{2}\left\{\dot{q}'\right\}^T[M']\left\{\dot{q}'\right\} - \frac{1}{2}\left\{q'\right\}^T[K']\left\{q'\right\} \tag{36}$$

where $\left\{q'\right\}$ is a column vector of independent coordinates. The substitution of equation (36) into Lagrange's equation (eq. (16)) yields

$$[M']\left\{\ddot{q}'\right\} + [K']\left\{q'\right\} = \left\{0\right\} \tag{37}$$

as the free-vibration equations of motion for the assembled structure. Equation (37) is seen to be of the same form as equation (17).

It has already been pointed out that the matrix $[C]$ is characterized by the presence of many null (zero) columns. The product $[D] = [C][U]$, however, does not generally contain any null columns. Hence, the procedure outlined in the appendix cannot be employed to reduce the order of the eigenvalue problem given by equation (32). However, the fullness of this matrix in no way detracts from the usefulness of the method of Walton and Steeves when applied in a component-mode synthesis formulation since the order of the matrix $[E']$, being equal to the number of component modes employed in the synthesizing procedure, is usually much less than the order of $[E]$ obtained in the direct method.

The preceding development has explicitly considered only the case of undamped free vibrations. However, the procedure can be extended to the more general case in which damping and external forces are included.

Some Additional Comments on the Method of Component-Mode Synthesis

Origin of component-mode shapes.- In order to perform the synthesis, the modal mass matrix $[\mathcal{M}]^{(i)}$, the modal stiffness matrix $[\mathcal{K}]^{(i)}$, and the mode shape matrix $[U]^{(i)}$ corresponding to each substructure must be known (cf., eqs. (21), (22), and (25)). Within the context of the present development these matrices can be established in several ways.

The substructure mass and stiffness matrices $[m]^{(i)}$ and $[k]^{(i)}$ can be formally established as an integral part of the computational procedure and used to calculate the substructure modes. From these modes a subset, augmented by any static or assumed shapes, is selected and assembled into $[U]^{(i)}$. The matrices $[\mathcal{M}]^{(i)}$ and $[\mathcal{K}]^{(i)}$ then follow from equation (22).

The present computational procedure can also incorporate the representation of individual substructures which have been analyzed by other engineering groups. If $[m]^{(i)}$, $[k]^{(i)}$, and $[U]^{(i)}$ are available from some external source, equations (22a) and (22b) can be used to determine $[\mathcal{M}]^{(i)}$ and $[\mathcal{K}]^{(i)}$. Considerable computational convenience can be realized, however, if the substructures are defined by a truncated set of orthogonal modes and their associated generalized masses and natural frequencies, since in this case there is no need to determine $[m]^{(i)}$ and $[k]^{(i)}$ explicitly. The modal mass and stiffness matrices $[\mathcal{M}]^{(i)}$ and $[\mathcal{K}]^{(i)}$ are both diagonal in this case. The set of generalized masses is assembled to give $\left[\diagdown\mathcal{M}\diagdown\right]^{(i)}$; $\left[\diagdown\mathcal{K}\diagdown\right]^{(i)}$ follows from

$$\left[\diagdown\mathcal{K}\diagdown\right]^{(i)} = \left[\diagdown\Omega^2\diagdown\right]^{(i)}\left[\diagdown\mathcal{M}\diagdown\right]^{(i)} \tag{38}$$

where $\left[\diagdown\Omega^2\diagdown\right]^{(i)}$ is a diagonal matrix containing the squares of the natural frequencies of the ith component on the main diagonal.

The definition of a substructure can also be based either partially or wholly on data obtained from a ground vibration test. If a set of orthogonal modes and associated frequencies for the ith component has been determined experimentally and the mass matrix $[m]^{(i)}$ is known, the generalized mass matrix for the ith substructure is given by

$$\left[\mathcal{M}\right]^{(i)} = [U]^{(i)^T}[m]^{(i)}[U]^{(i)} \tag{39}$$

and the generalized stiffness matrix follows from equation (38). Note that in this case only the stiffness matrices of the components are not required. Alternately, the generalized masses, and hence $\left[\mathcal{M}\right]^{(i)}$, could be obtained experimentally by means of the displaced frequency technique (ref. 27). The generalized stiffness matrix then follows easily from equation (38). It should be pointed out, however, that in practice it may not be possible to determine experimentally a sufficient number of generalized masses with accuracy; in such cases, the mass properties of the substructures must be known and $\left[\mathcal{M}\right]^{(i)}$ must be determined by means of equation (39).

Simultaneous use of discrete and modal coordinates.- Various aircraft appendages, such as engine-nacelle combinations, ordnance, external fuel tanks, and so on, can often be treated as rigid bodies in dynamic analyses. The inertial properties of such components can be conveniently introduced in the form of lumped values for the mass and for the moments and products of inertia relative to some axes fixed to the center of mass of the item. Conversely, other structural members such as pylons, landing-gear struts, control surface actuators, and so on, can frequently be adequately treated as springs in dynamic analyses. When such structural members are identified as substructures in a modal synthesis formulation, no modal expansion is associated with them. In order to accommodate the components idealized in this manner, the modal expansion matrices $[U]^{(i)}$ (cf. eq. (18)) corresponding to such substructures are taken to be unit matrices $[I]^{(i)}$ and their expansion given by

$$\{p\}^{(i)} = [I]^{(i)}\{\xi\}^{(i)} \tag{40}$$

where the order of $[I]^{(i)}$ is equal to the number of degrees of freedom of the rigid body or spring substructure. It is possible to use an "identity expansion" of the form given in equation (40) for any substructure by setting the order of $[I]^{(i)}$ equal to the number of discrete degrees of freedom of the substructure. This expedient provides the basis for what might be termed a hybrid method of analysis in which some substructures are described in terms of discrete coordinates while the remaining substructures are described in terms of modal coordinates. Such a simultaneous use of both discrete and modal coordinates may be useful in practice.

It is interesting to note that if $[U]$ in equation (19) is taken to be a unit matrix $[I]$ of order $N \times N$, the component-mode synthesis formulation becomes numerically identical to that of the direct method. Hence, as formulated herein, the direct method is a special case of component-mode synthesis.

Solution of Equations of Motion

Transformation of generalized eigenvalue problem to standard eigenvalue form.- The free-vibration equations of motion resulting from the application of either the direct or component-mode synthesis methods have the matrix form

$$[M]\{\ddot{q}\} + [K]\{q\} = \{0\} \tag{41}$$

where $[M]$ and $[K]$ are symmetric, full, and (possibly) singular. The singularity of $[M]$ is associated with the presence of zero masses in the substructure mass matrices either as a consequence of setting to zero certain mass terms (e.g., rotary inertias) or as a consequence of the introduction of auxiliary coordinates (having no mass) to provide points of connection with other components. The stiffness matrix $[K]$ is singular if the structure is unrestrained either internally (i.e., has internal linkages) or externally (i.e., the system moves as a rigid body). Mathematically, $[M]$ and $[K]$ are termed positive semidefinite, a term which means that the eigenvalues of $[M]$ and $[K]$ are greater than or equal to zero (ref. 28).[6] A matrix which is positive definite has eigenvalues which are all positive and is thus nonsingular. A matrix which is semidefinite has one or more zero eigenvalues and is thus singular.

With the assumption of a solution of the form $\{q\} = \{q_o\}e^{i\omega t}$, equation (41) assumes the familiar form

$$[K]\{q_o\} = \omega^2[M]\{q_o\} \tag{42}$$

by removal of the time factor $e^{i\omega t}$. In order to take advantage of the algorithms available for the solution of the eigenvalue problem in standard form (ref. 29), it is the usual practice to reduce equation (42) to the standard form

$$[A]\{x\} = \lambda\{x\} \tag{43}$$

---

[6]Stated physically, the kinetic and potential energy of a linear conservative system can never be negative.

If $[M]$ (or $[K]$) is nonsingular, equation (42) can be reduced to this form by simply multiplying through by the inverse of $[M]$ (or $[K]$), in which case λ would be identified with ω^2 (or $1/\omega^2$). The matrix $[A]$ established in this manner would, in general, be nonsymmetric. Since there are several attendant numerical advantages which may be realized if the problem is formulated in symmetric eigenvalue form (cf. refs. 30 and 31), an alternative approach would be to reduce equation (42) to the form of equation (43) in a manner which leads to a matrix $[A]$ which is symmetric. Procedures for solving either the symmetric or nonsymmetric eigenvalue problem are well documented in the literature (refs. 29 to 35).

Since $[K]$ is singular in any vibration analysis of a structure having unrestrained degrees of freedom, the reduction of the generalized eigenvalue problem given in equation (42) to standard symmetric form is usually based on the assumption that $[M]$ is nonsingular. Then either a Cholesky decomposition procedure (ref. 7) or the eigenvectors of the mass matrix (ref. 32) are employed in a coordinate transformation to reduce $[M]$ to a diagonal matrix. In general, however, $[M]$ may also be singular and these procedures are not applicable. If the mass matrix in equation (41) were diagonal, the singularity of $[M]$ would be reflected by one or more zero elements on the diagonal of $[M]$; thus, equation (42) could easily be cast into a partitioned form which is amenable to static condensation of the massless degrees of freedom (ref. 36). The mass matrix in equation (41) is a full matrix, however, and the singularity of $[M]$ is not evidenced by the presence of null rows and columns of $[M]$. Hence $[M]$ cannot be cast into the partitioned form required for static condensation of the massless coordinates. A practical procedure for transforming equation (42) to standard symmetric form, in the case where both $[M]$ and $[K]$ are singular and $[M]$ is not diagonal has been given by Walton and Durling (unpublished work, 1966) and has been implemented in a NASA Langley Research Center computer program designated BJD5. In their procedure the mass matrix is first diagonalized by a modal transformation as suggested in reference 32. The zero diagonal elements are then eliminated by the condensation procedure given in reference 36. Since their method is adopted in the present work, the analytical basis of their procedure is reviewed here for completeness.

The initial step in the procedure of Walton and Durling is the solution of the mass eigenvalue problem; that is, the solution of

$$[M]\{x\} = \mu\{x\} \tag{44}$$

for all its eigenvalues and eigenvectors. The matrix $[M]$ in equation (42) can then be reduced to a diagonal matrix $\lceil \mu \rfloor$ through the orthogonality transformation

$$[Q]^T[M][Q] = \lceil \mu \rfloor \tag{45}$$

The matrix $[Q]$ is a square matrix the columns of which are the eigenvectors of equation (44) and the diagonal elements of $\lceil \mu \rfloor$ are the corresponding eigenvalues. Formally, this reduction is carried out by substituting the coordinate transformation

$$\{q_o\} = [Q]\{\eta\} \tag{46}$$

into equation (42) and premultiplying by $[Q]^T$. This substitution gives

$$[Q]^T[K][Q]\{\eta\} = \omega^2[Q]^T[M][Q]\{\eta\} \tag{47}$$

or

$$[S]\{\eta\} = \omega^2\lceil \mu \rfloor\{\eta\} \tag{48}$$

where the definition of $[S]$ follows from equation (47). If $[M]$ is singular one or more of its eigenvalues is zero. It is assumed that all of the eigenvalues which are zero are grouped so that they constitute the lower diagonal elements of the matrix $\lceil \mu \rfloor$. This arrangement is a natural consequence of any eigenvalue routine which arranges the eigenvalues in descending order according to magnitude, such as the Jacobi method (ref. 30) employed in BJD5. Otherwise, an appropriate rearrangement of rows and columns must be carried out. In either case equation (48) can then be written in the partitioned form

$$\left[\begin{array}{c|c} [S_{11}] & [S_{12}] \\ \hline [S_{21}] & [S_{22}] \end{array}\right]\left\{\begin{array}{c} \{\eta_1\} \\ \hline \{\eta_2\} \end{array}\right\} = \omega^2\left[\begin{array}{c|c} \lceil \mu_1 \rfloor & [0] \\ \hline [0] & [0] \end{array}\right]\left\{\begin{array}{c} \{\eta_1\} \\ \hline \{\eta_2\} \end{array}\right\} \tag{49}$$

where $\lceil \mu_1 \rfloor$ is a nonsingular diagonal matrix containing the eigenvalues of $[M]$ which are not zero. The inertia matrix on the right-hand side of equation (49) is now in the form required to effect a static condensation (ref. 36). The application of static condensation to the "inertialess" coordinates $\{\eta_2\}$ yields

$$[\tilde{S}]\{\eta_1\} = \omega^2\lceil \mu_1 \rfloor\{\eta_1\} \tag{50}$$

where $[\tilde{S}]$ is the reduced stiffness matrix given by

$$[\tilde{S}] = \Big[[S_{11}] - [S_{12}][S_{22}]^{-1}[S_{21}] \Big] \tag{51}$$

and $\left\lceil \mu_1 \right\rfloor$ is the reduced mass matrix. Since $[S_{11}]$ and $[S_{22}]$ are symmetric and $[S_{21}]$ is the transpose of $[S_{12}]$, the reduced stiffness matrix given by equation (51) is symmetric. Since all the submatrices of the original generalized stiffness matrix appear in $[\tilde{S}]$ and all the submatrices of the original generalized mass matrix appear in $\left\lceil \mu_1 \right\rfloor$, the eigenvalue problem is preserved (ref. 37). The final step in the reduction procedure consists of reducing $\left\lceil \mu_1 \right\rfloor$ to a unit matrix using the coordinate transformation

$$\{\eta_1\} = \left\lceil \frac{1}{\sqrt{\mu_1}} \right\rfloor \{\hat{\eta}_1\} \tag{52}$$

If equation (52) is substituted into equation (50) and is premultiplied by $\left\lceil \frac{1}{\sqrt{\mu_1}} \right\rfloor$, the result is

$$\left\lceil \frac{1}{\sqrt{\mu_1}} \right\rfloor [\tilde{S}] \left\lceil \frac{1}{\sqrt{\mu_1}} \right\rfloor \{\hat{\eta}_1\} = \omega^2 [I] \{\hat{\eta}_1\} \tag{53}$$

or, finally,

$$[\hat{S}]\{\hat{\eta}_1\} = \omega^2 \{\hat{\eta}_1\} \tag{54}$$

where $[\hat{S}]$ is symmetric.[7]

An alternate final form for the eigenproblem, in which the eigenvalues are the reciprocals of the squares of the natural frequencies, could also be established within the context of this development. In order to arrive at such a form, the preceding matrix manipulations would be modified only to the extent that the roles of $[M]$ and $[K]$ from equation (44) onward would be reversed. If such an interchange were made the final equations would assume the form

---

[7]More recently, a procedure for reducing the general eigenvalue problem to standard symmetric form has also been given by Peters and Wilkinson (ref. 38).

$$[\underline{S}]\{\underline{\eta}_1\} = \frac{1}{\omega^2}\{\underline{\eta}_1\} \tag{55}$$

A reduction to this alternate form is not included as an option in BJD5 but is only mentioned here for completeness.

Interpretation of eigensolutions.- Solution of the eigenvalue problem given in equation (54) leads to a set of eigenvalues ω_i^2 and associated eigenvectors $\{\hat{\eta}_1\}_i$. Since eigenvalues are invariant under orthogonality transformations such as those employed in reducing equation (42) to the form given in equation (54), the ω_i^2 are squares of the desired system natural frequencies. However, the eigenvectors $\{\hat{\eta}_1\}_i$ are generalized mode shapes and must be transformed back to the original coordinates $\{z\}_i$ for physical interpretation. For the direct method this back transformation is given by

$$\{z\}_i = [\beta][Q]\begin{bmatrix} [I] \\ -[S_{22}]^{-1}[S_{21}] \end{bmatrix}\begin{bmatrix} \diagdown \frac{1}{\sqrt{\mu_1}} \diagdown \end{bmatrix}\{\hat{\eta}_1\}_i \tag{56}$$

For component-mode synthesis the back transformation is

$$\{z\}_i = [U][\beta'][Q']\begin{bmatrix} [I] \\ -[S_{22}']^{-1}[S_{21}'] \end{bmatrix}\begin{bmatrix} \diagdown \frac{1}{\sqrt{\mu_1'}} \diagdown \end{bmatrix}\{\hat{\eta}_1'\}_i \tag{57}$$

where the primes have been reintroduced for the purpose of distinguishing between common symbols representing matrix quantities which are different numerically. It should be noted that the nodal deflections at the massless degrees of freedom are recovered in the back transformation.

The final mode shapes $\{z\}_i$, as given by equations (56) and (57), are all normalized to unit generalized mass. This particular normalization is a direct consequence of reducing the general eigenvalue problem to a standard form which is symmetric using a transformation which reduces $[M]$ to a unit matrix rather than $[K]$. It should also be noted that these mode shapes are given in terms of the local coordinates established during the discretization of the substructures rather than in terms of a single set of coordinates appropriate to some global axis system.

Comments on solution of eigenproblems appearing in formulations.- Several eigenproblems require solution during vibration analysis by either the direct or component mode synthesis methods as previously outlined. Two of these problems, the eigenproblem formed from the coefficient matrix of the constraint equations (eqs. (11) and (32)) and the eigenproblem for the mass matrix (eq. (44)), require the computation of all the eigenvalues and eigenvectors of full matrices. Since these matrices are symmetric, Jacobi's method (refs. 30 to 32) is directly applicable and leads to all eigenvalues and eigenvectors simultaneously. Another general-purpose approach to the solution of the complete eigenproblem is either Givens' or Householder's method. This approach transforms the matrix to tridiagonal form (refs. 31 and 34) followed by the QR transformation (refs. 30, 31, and 35) to obtain the eigenvalues. The associated eigenvectors are then obtained through inverse iteration (refs. 30, 34, and 35). Both of the preceding approaches can also be employed in the solution of the final eigenproblem as given in either equation (54) or (55). The numerical effort required to solve the final eigenvalue problem in either form can be reduced if only the eigenvalues (and corresponding eigenvectors) of interest are computed. For example, with the use of equation (55) some variant of the power method in combination with matrix deflation (refs. 30 to 33) could be employed to solve for only the largest eigenvalues corresponding to the lowest frequency modes of interest. Alternately, the use of the Sturm-sequence property in conjunction with bisection (refs. 30, 31, 33, and 34) can be applied to either equation (54) or (55) to determine the eigenvalues of interest. Inverse iteration would then be used to obtain the corresponding eigenvectors. Detailed considerations of these procedures for solving the matrix eigenvalue problem in standard form are contained in the cited references. Several algorithms which deal with the eigenvalue problem in the form given by equation (42) have also appeared in the literature. (See, for example, refs. 35 and 39.) These latter methods solve directly for the eigenvalues and eigenvectors without a transformation to standard form.

The computer implementation of the reduction procedure of Walton and Durling in BJD5 is based on the use of Jacobi's method for solving both the mass eigenvalue problem and the final eigenproblem in the form given by equation (54). The Jacobi method is also employed to solve the constraint eigenvalue problem in the implemented versions of the direct and component-mode synthesis formulations. A variant of BJD5 is employed to calculate the component modes which are generated internal to the implemented version of the modal synthesis procedure. Thus, Jacobi's method is used to solve all the eigenproblems which occur in the computer implementation of the procedures described. It should be emphasized that Jacobi's method is particularly appropriate for solving the constraint and mass eigenvalue problems. With respect to the constraint eigenvalue problem, recall that the identification of a suitable transformation matrix from dependent to independent coordinates by the method of Walton and Steeves requires that the eigenvectors corresponding to the zero eigenvalues be linearly independent. The Jacobi method appears to be the only algorithm which avoids the numerical problems and special considerations associated with determining linearly independent eigenvectors corresponding to equal eigenvalues; the resulting eigenvectors are almost exactly orthogonal and provide full digital accuracy (ref. 30). With regard to the mass eigenvalue problem, the eigenvectors (assumed to be orthogonal) are used to establish a transformation matrix which serves to diagonalize the mass matrix. Since $[M]$ can be singular and have more than one zero eigenvalue, the use of the Jacobi method not only minimizes the numerical problems associated with determining linearly independent eigenvectors corresponding to equal eigenvalues but also obviates the need to apply any type of orthogonalization procedure to the computed eigenvectors.

NUMERICAL RESULTS: ANALYTICAL AND EXPERIMENTAL VERIFICATION OF ANALYSES

The computational procedures for natural mode analysis by the direct and component-mode synthesis techniques developed herein have been implemented in two special-purpose computer programs – SUDAN and SCORE. The SUDAN program is intended for structures which can be represented as an equivalent system of beam, spring, and rigid-body substructures. A combined lumped-mass/finite-element stiffness technique is used to model each of the substructures comprising the system. The SCORE program, however, is more general in that it provides for the use of both internally and externally generated substructure modal information either separately or in combination. Modal properties generated internally to the SCORE system are based on the same modeling which is used in SUDAN. Modal properties of substructures generated external to the SCORE system can be based on any type of finite-element analysis, the required input data being a truncated set of orthogonal modes and the corresponding natural frequencies and generalized masses. This latter feature thus provides for the direct use of substructure modes which may have been calculated by different engineering groups or analyses based on more sophisticated mathematical models.

Some comparative studies based on the application of the direct and component-mode synthesis procedures to a free-free beam and a collection of beams configured in the shape of an airplane are presented first. A comparison of the theoretical solutions with experimentally measured modes and frequencies of the airplane beam assembly is also shown. The next application shown has reference to a 1/15-scale dynamic model of an early space shuttle concept where experimentally measured frequencies are compared with those obtained from the present component-mode synthesis analysis as well as from two other different analyses. These results point out the importance of properly modeling the interfaces between substructures. The last application considered has reference to a comparison of the modes and frequencies measured on a 1/30-scale dynamic aeroelastic model of a B-52E airplane with those modes and frequencies obtained from an analysis by the direct method.

Free-Free Beam

Some comparative analytical studies for the purpose of assessing the accuracy of partial modal synthesis are based on considerations of the free-free bending modes and frequencies of a uniform beam having the following properties:

L = Total length, 137.16 cm (54 in.)

M = Total mass, 13.28 kg (0.07587 lb-sec^2/in.)

EI = Bending stiffness, 1434.9 kN-cm^2 (50 000 lb-in^2)

$$\frac{I}{A} = \frac{\text{Section moment of inertia}}{\text{Area of cross section}}, \; 188.13 \text{ cm}^2 \; (29.16 \text{ in}^2)$$

In order to provide a basis for comparison, the beam eigenvalue problem was first formulated and solved as if it were a single beam represented by a finite-element model consisting of nine elements. The distributed mass and rotary inertia were lumped at 10 equally spaced stations along the lengthwise axis of the beam as shown in the sketch at the top of table I. Each station had 2 degrees of freedom, vertical translation and rotation, for a total of 20 degrees of freedom. For the modal synthesis analysis the beam was divided into three unequal-length segments having 8, 6, and 10 degrees of freedom, respectively, according to the lower sketch in table I. Since continuity must be preserved in both translation and rotation at each of the two connection points, there are four equations of constraint. A summary of the physical properties of these lumped-mass systems is also given in table I.

Frequencies obtained by direct analysis of the complete beam, by full modal synthesis, and by four combinations of partial modal synthesis employing subsets of the lower modes from each beam segment are compared in table II. Full modal coupling using all 24 of the component modes gives results which are identical to those obtained by the direct method. The direct results are taken as the basis for assessing the accuracy of the results obtained by partial modal synthesis. The frequency results shown in table II indicate that the accuracy of the synthesis results decreases as the number of component modes used in the synthesizing procedure is reduced. It is interesting to note that even in the extreme case in which only three modes from each beam segment are used (one elastic mode and two rigid-body modes) the three predicted elastic-mode frequencies still compare favorably with those given by the direct method. In figure 4 comparison is made of the mode shape displacements in the first four elastic modes as obtained from the direct method and partial modal synthesis (employing half of the modes from each beam segment). In order to provide for a more critical comparison of the mode shapes, the actual computed displacements and slopes for the fourth elastic mode resulting from direct analysis, for full modal coupling, and for two combinations of partial modal synthesis are given in table III. The results of full modal synthesis are in agreement with the direct results through the eight significant figures shown. As the number of component modes used decreases, the degradation in accuracy of the modal-synthesis results is again evident.

Airplane Beam Assembly

Both the direct and component-mode synthesis methods of analysis have been applied to a model consisting of an assembly of beams configured in the shape of an airplane and the results compared with experimental modes and frequencies. This model is shown in figure 5 as it appeared during the shake test. Figure 6 summarizes the geometric properties of the model. The analysis was restricted to symmetric motions. The motions of interest were fuselage pitch bending and wing and tail vertical bending and torsion. The distributed mass of the fuselage, wing, and tail beams was lumped at discrete points along the elastic axes of the respective members. Each fuselage station had two degrees of freedom: vertical translation and rotation. In addition to these two degrees of freedom, each wing and tail station also had a torsional degree of freedom. Each member was also allocated a rigid-body degree of freedom directed along its lengthwise axis. The rotary inertia associated with each lumped mass was assumed unimportant and taken to be zero. The model properties, as discretized for the analyses, are summarized in table IV. There were 68 degrees of freedom associated with the uncoupled system; 26 of the 68 corresponded to massless coordinates as a consequence of neglecting rotary inertia. The results of some comparative studies pertaining to this model are summarized in figures 7 and 8 and in tables V and VI. The results shown for partial modal synthesis are for a single combination of the lowest component modes. In addition to the component rigid-body modes the synthesis included: the 6 lowest fuselage modes, the 5 lowest wing modes (3 bending and 2 torsion), and the 2 lowest tail modes (1 bending and 1 torsion) for a total of 21 modes (8 rigid body and 13 elastic). The wing and tail modes corresponding to clamped-free, pinned-free, and free-free end conditions were used in conjunction with the free-free fuselage modes. These combinations are employed to provide an indication of the type of wing and tail component modes which lead to results most nearly in agreement with those obtained from the direct analysis.

An assessment of the accuracy of the direct analysis was made by comparing the results obtained by this method with those obtained experimentally. The frequency comparison given in table V is quite good in view of the rather coarse spacing between stations on the fuselage and wing. The corresponding comparison of the mode shapes is made in figure 7. Excellent agreement is shown through the highest mode for which experimental results were available (the seventh elastic mode).

With the results of the direct analysis as a reference, the results given for partial modal synthesis in table V and figure 8 show that best agreement is achieved when clamped-free modes are employed for the wing and tail. This agreement is a consequence of the fact that those modes are based on root conditions which more closely resemble the conditions existing in the coupled structure than either the free-free or pinned-free modes. A more critical comparison of the modes than that shown in figure 8 is made in table VI where the calculated values for the sixth mode (the fourth elastic mode) are displayed.

An inspection of the first two result columns in tables V and VI indicates that the results obtained by full modal synthesis do not agree exactly with those obtained by direct analysis. This lack of agreement is in contrast to a similar comparison made for the case of the free-free beam in tables II and III. The "discrepancy" in the present case is a consequence of the fact that while all the calculated component modes were used in the synthesizing procedure, the component-mode sets $[U]^{(i)}$ were not complete; that is, the number of component modes was less than the number of substructure elastic degrees of freedom.[8] This "modal defect" is attributable to the presence of massless degrees of freedom (specifically, the rotary inertias which were set to zero) in the equations of motion. Mathematically, the component mode sets $[U]^{(i)}$ employed in the "full" modal synthesis did not span the finite dimensional space of each substructure (ref. 40). Hence, the component-mode sets did not constitute a basis set of vectors for expressing any general component displacement vector $\{p\}$ having N elastic degrees of freedom as a linear combination of $n(n < N)$ component modes calculated in the presence of zero masses. This deficiency in the number of modes is equivalent to placing constraints on the system (ref. 41); these constraints should tend to give frequencies which are higher than those obtained from the direct analysis. This frequency shift is apparent in table V. A complete set of component modes (actually, any linearly independent set of shapes which spans the component vector space) is needed to fulfill the requirement for full modal coupling. For convenience, a complete set of such shapes was established in this case by calculating the component "modes" with the assumption of the arbitrary value of 1.153 kg-sec^2-cm (1.0 lb-sec^2-in.) for all the degrees of freedom having zero inertia. This artifice was employed only to arrive at a complete set of linearly independent shapes for each substructure; the assumed inertias were not retained in $[\overline{M}]$ during the subsequent synthesizing procedure. The results obtained using these "quasi-component modes" in a full modal synthesis are given in the columns having the heading "Quasi-

[8]The number of elastic degrees of freedom for the fuselage, wing, and tail is 26, 21, and 18, respectively, while the number of calculated component modes is 13, 14, and 12, respectively.

component modes" in tables V and VI. It should be noted that these particular results are in exact agreement with those of the direct analysis. Hence, full modal synthesis may be regarded as "exact" in the case of a finite degree-of-freedom system when the number of linearly independent shapes employed in the synthesizing procedure equals the number of discrete elastic degrees of freedom.

Space Shuttle Model

In order to evaluate modal synthesis techniques for dynamic analysis of coupled systems like the space shuttle, companion experimental and analytical studies were conducted on a 1/15-scale dynamic model of an early shuttle concept consisting of a booster and an orbiter (ref. 42). The model consisted of a pair of tubular-type beams arranged in a parallel "piggy-back" fashion and joined together by two spring assemblies as shown in figure 9. This figure actually shows the model in a configuration employed in another investigation in which the wing structures shown in the photograph were present. The study of reference 42 did not include these wing structures. A cable suspension system (partially visible in fig. 9) was employed to simulate a "free-flight" condition.

The results obtained for vibrations in the pitch plane using the modal synthesis scheme described herein as well as two other analyses are compared with the experimental results in figure 10. The analytical results correspond to three different investigations in which the mathematical models differed as to their idealization of the booster and orbiter structures. All three investigations used the same mathematical modeling of the spring assemblies (the interfaces between the booster and orbiter) but used different attachment conditions for the connections with the booster and orbiter. The model with pinned connections was employed by a contractor to evaluate a specific modal coupling procedure. The model with fixed connections employed NASTRAN (NASA STRuctural ANalysis) in a direct analysis of the complete model (ref. 43). The model with flexible rotational connections was analyzed by the modal synthesis procedure of this report as implemented in computer program SCORE. The analytical results shown for the flexible interface model are based on using eight booster modes and seven orbiter modes; each group consisted of a mixture of free-free elastic modes, rigid-body modes, and assumed static deflection shapes.

The agreement between the measured and calculated frequencies is good for all three analyses, except for the fourth mode. The mathematical model with the pinned connections on the springs did not allow for coupled axial motions and therefore could not predict this mode, which had significant axial motion. The model with the rigid connections for the interfaces, while allowing the coupling between beam bending and axial motion, introduced too much rotational stiffness and severely overpredicted the frequency of the fourth mode. The results shown for the model with flexible interface connections were obtained by adjusting the value of the connecting rotational spring stiffness in the analysis until the frequency of the mode agreed with the experimental value. A comparison of the corresponding calculated mode shape with the experimental shape is made at the bottom of figure 10.

Since the analytical results of figure 10 are based on three different idealizations of the booster and orbiter structures, they are not intended to provide a basis for the comparison of the accuracy of the corresponding analyses. Rather, the analytical results are intended to illustrate the importance of correctly modeling the interface conditions between substructures. The interested reader is referred to reference 42 for further details and discussion.

B-52 Aeroelastic Model

A 1/30-scale dynamic aeroelastic model of a B-52E airplane is being employed in a Langley Research Center wind-tunnel research program to investigate the use of active controls for gust alleviation. The model design specification requirements (ref. 44) stipulated that dynamic simulation of the first eight symmetric free-free elastic modes and frequencies be maintained. Verification of this model design was accomplished by comparing measured modes and frequencies with those obtained from an analysis by the direct method by means of a special-purpose B-52 computer program specifically written to treat only the configuration of this model.[9] Upon completion of the initial gust-response studies the model was modified to represent a different gross-weight condition and was then employed in a study of a model flutter-suppression system (ref. 45). Design verification of the modified model was again established by comparing the measured modes and frequencies with those obtained from an analysis by the direct method as implemented in the special-purpose B-52 program as well as in the SUDAN program. The analytical modes were also employed in a model flutter analysis. The results of this particular modal comparison are shown in this section.

The 1/30-scale model, as it appeared during the shake test, is shown in figure 11. The model was supported at its center of gravity by a soft spring such that the support frequency was about 1/8 the frequency of the first elastic mode. Details of the model construction are shown in figure 12 which gives two views of the model with several of the segmented shell structures removed; these structures provide the external aerodynamic shape. The representation of the model as an equivalent system of beam, spring, and rigid-body components for the vibration analysis is depicted in figure 13. The fuselage and wing structures were replaced by nonuniform beams lying along the elastic axes of the respective components. Since the fuselage structure had two discontinuities in its elastic axis, three beams were used to represent the fuselage structure, with the coupling

[9]Unpublished work of William C. Walton, Jr., Barbara J. Durling, and Raymond G. Kvaternik. The computer program was written by Barbara J. Durling.

joints between the beams assumed to be rigid. The tip tank and the empennage were treated as rigid and were rigidly connected to the components adjacent to them. The nacelles were treated as rigid and the nacelle pylons were modeled as springs. The mass of the pylons was distributed to the local wing structure and to the nacelles to which they were attached.

For the beam model shown in figure 13 the mass and stiffness matrices for the partitioned structure ($[\overline{M}]$ and $[\overline{K}]$ of eq. (3)) have the general form indicated in figure 14. Each block in figure 14 corresponds to a submatrix. The ordering of these submatrices within the larger substructure submatrices (indicated by braces) and the ordering of the substructure submatrices within $[\overline{M}]$ and $[\overline{K}]$ must be compatible; the ordering is otherwise arbitrary. Since the mass and stiffness matrices for each substructure are generated independently, no intersubstructure coupling exists in $[\overline{M}]$ or $[\overline{K}]$. However, intrasubstructure coupling (i.e., coupling between submatrices within a substructure submatrix through off-diagonal terms) can exist. For example, if the sectional centers of gravity of the wings were displaced from the wing elastic axis in the plane of the wings, mass static unbalance terms would appear outside the block diagonal areas and couple the vertical bending and torsion submatrices in each of the wing substructures in $[\overline{M}]$. In the present case, the bending-torsion coupling induced by wing mass unbalance is negligible compared to the coupling induced by the nacelles and tip tanks; hence, the wing mass unbalance has been assumed to be zero. Therefore, no such coupling is indicated in figure 14.

The measured frequencies and node lines for the first eight symmetric elastic modes are compared with results obtained by the direct method of analysis in figure 15. Since the structural properties of the left-hand and right-hand wings and appendages differed slightly, node lines are shown for both wing surfaces in order to provide an indication of the effects on the mode shapes of the structural asymmetry inherent in the model. The analytical results are based on the use of values which are an average of the left- and right-hand-side properties. Deviation of the calculated frequencies from the measured values varies from a maximum of 11.2 percent in the third mode to a minimum of 0.80 percent in the eighth mode. The theoretical node lines for the wing surfaces are generally in agreement with the experiment; the exception is the fourth mode. However, several disparities exist between the theoretical and experimental fuselage node lines for the third, fourth, and fifth modes. The seventh vibration mode could not be isolated because of the presence of a dominant antisymmetric mode at 15.7 hertz. Several aspects of the model construction which were not accounted for in the mathematical model were thought to be the cause of the discrepancies. The segmented balsa-fiberglass shell structures enclosing the fuselage and wing beams to provide the external aerodynamic shape were intended to contribute negligible stiffness to the fuselage and wing-beam structures. However, an inspection of the model indicated that the existing shell structures did, in fact, contribute significant stiffness in the region of the wing-body juncture and, to a lesser extent, elsewhere. The actuator rods for the flaperons, ailerons, horizontal tail, and elevator, being continuous and passing through several shell segments (see fig. 12), were also identified as likely sources of additional stiffness. In light of these considerations, the stiffnesses of the fuselage and wing beams used in the analysis were arbitrarily increased (the largest increase being applied in the region of the fuselage-wing juncture) and the modes and frequencies recalculated. Although these results are not shown, it should be remarked that the introduction of these stiffness adjustments brought the calculated fuselage nodes in the third and fifth modes into agreement with experiment; the good agreement in the other wing and body node lines in these two modes was not affected. The adjustments also had a negligible effect on the nodal patterns in the other modes. In all cases only small changes in frequency were noted. The stiffness adjustments did not bring the fourth mode shape into agreement with experiment. However, the experimental definition of this mode was itself questionable because the closeness of its frequency to that of the third mode, in conjunction with an inability to excite the mode sufficiently, precluded a reliable identification of the node lines.

The usefulness of the modes calculated without any adjustments in stiffness was demonstrated in subsequent flutter analyses. The dynamic pressure, frequency, and mode shape at flutter were correctly predicted by the analyses.

Although component-mode synthesis was not employed in the B-52 model vibration analysis, it is of interest to indicate the general form of the uncoupled system modal expansion matrix $[U]$ (cf. eqs. (18) and (19)) corresponding to the beam representation given in figure 13. For the substructuring order given in figure 14, this matrix would have the form shown in figure 16. In addition to indicating the block diagonal composition of $[U]$, this figure also illustrates the use of the "identity expansion" (see eq. (40)) for both spring and rigid-body substructures and for substructures which are treated as rigid in one direction and elastic in another.

CONCLUDING REMARKS

Two computational procedures for calculating the natural vibratory modes and frequencies of complex structural systems have been presented. Both procedures are based on a substructures methodology and both employ the finite-element stiffness method to model the constituent substructures. The first procedure described was a direct method based on solving the matrix eigenvalue problem associated with a finite-element model of the complete structure. The second procedure described was a component-mode synthesis scheme whereby the vibration modes of the complete structure are synthesized from modes of substructures into which the structure has been divided. The latter method was shown to provide for a significant reduction in the number of degrees of freedom through the expedient of partial modal synthesis wherein only a truncated set of the modes corresponding to each substructure is employed in the synthesizing procedure.

The computational procedures presented contain a combination of features which enhance their generality and utility. Specifically, both methods assemble the structure by imposing the compatibility relations on the substructure attachment coordinates according to an algorithm devised by Walton and Steeves. A nondiagonal mass matrix can be accommodated in both methods. The general case in which the system mass and stiffness matrices are both singular is also admitted. Additional features which are incorporated in the component-mode synthesis formulation include: a hybrid coordinate representation whereby both modal and discrete coordinates can be employed simultaneously; component-mode shapes which are completely arbitrary with respect to their origin, type, and normalization; a unified treatment of the component shapes in the synthesizing procedure without recourse to matrix partitioning according to the type of component modes employed. The combination of these features in a direct and component-mode synthesis formulation is thought to be new and to provide the basis for computational procedures which are unique with respect to their generality, computational convenience, and ease of computer implementation.

The results of the application of SUDAN (SUbstructuring in Direct ANalysis) and SCORE (Synthesis of COmponent REsponses) (the computer implementation of these computational procedures) to several structural configurations were shown. These results included: a free-free beam; an assembly of beams configured in the shape of an airplane; a 1/15-scale dynamic model of an early space shuttle concept; and a 1/30-scale dynamic, aeroelastic model of a B-52E airplane. Comparisons were also shown with experimental results for three of these configurations. These studies, as well as others for a variety of airframe dynamic analyses in support of various projects, have verified the analytical basis of these procedures and have demonstrated a wide range of engineering applicability for the SUDAN and SCORE programs.

Langley Research Center
National Aeronautics and Space Administration
Hampton, Va. 23665
July 10, 1975

APPENDIX

REDUCING THE ORDER OF THE CONSTRAINT EIGENVALUE PROBLEM IN THE DIRECT METHOD

Three eigenvalue problems require solution under vibration analysis by the direct method as outlined in the main body of this paper. The largest of these problems is that associated with the matrix product $[C]^T[C]$; $[C]$ is the matrix of coefficients of the constraint equations. There are often many coordinates (degrees of freedom) which do not appear in the constraint equations, a condition which leads to a matrix $[C]$ having many columns which are identically zero. Each such null column in $[C]$ will lead to a similarly positioned null column in the product $[C]^T[C]$ and a corresponding null row. Through an appropriate rearrangement of rows and columns, a significant reduction in the size of the eigenvalue problem which must actually be solved in such instances can be achieved.[10] The analytical basis on which such a reduction can proceed is given below.

From the constraint equations

$$[C]\{z\} = \{0\} \tag{A1}$$

the matrix $[E]$, defined as

$$[E] \equiv [C]^T[C] \tag{A2}$$

is formed and the associated eigenvalue problem

$$[E]\{x\} = \lambda\{x\} \tag{A3}$$

is solved. Let $[S]$ be a permutation matrix which, when postmultiplying $[C]$, rearranges the columns of $[C]$ so that all null columns are at the right. The construction of such matrices is discussed in references 2 and 30. The introduction of the transformation

$$\{x\} = [S]\{y\} \tag{A4}$$

---

[10]This possibility was pointed out to the author by William C. Walton, Jr. of NASA-Langley.

into equation (A3) and of the premultiplication by $[S]^{-1}$ gives

$$[S]^{-1}[E][S]\{y\} = \lambda[S]^{-1}[S]\{y\} \tag{A5}$$

With the definition of $[B]$ as

$$[B] \equiv [S]^{-1}[E][S] \tag{A6}$$

equation (A5) can be written as

$$[B]\{y\} = \lambda\{y\} \tag{A7}$$

Because of the rearranging properties of $[S]$, the transformation given by equation (A6) permits equation (A7) to be written in the partitioned form

$$\left[\begin{array}{c|c} [B_{11}] & [0] \\ \hline [0] & [0] \end{array}\right]\left\{\begin{array}{c} \{y_1\} \\ \hline \{y_2\} \end{array}\right\} = \lambda\left\{\begin{array}{c} \{y_1\} \\ \hline \{y_2\} \end{array}\right\} \tag{A8}$$

where $[B_{11}]$ is a square matrix of an order equal to the number of nonzero columns in $[C]$. When expanded, equation (A8) reduces to the two uncoupled eigenvalue problems,

$$[B_{11}]\{y_1\} = \lambda\{y_1\} \tag{A9a}$$

$$[0] = \lambda\{y_2\} \tag{A9b}$$

All the eigenvectors of $[B_{11}]$ can be assembled by columns into the matrix $[Y_1]$. The solutions to equation (A9b) are simply any set of linearly independent vectors (for example, the identity matrix $[I]$). These linearly independent vectors can be assembled by columns into the matrix $[Y_2]$. The matrix of eigenvectors associated with equation (A8) can then be written in the partitioned form

$$[Y] = \left[\begin{array}{c|c} [Y_1] & [0] \\ \hline [0] & [Y_2] \end{array}\right] \tag{A10}$$

The matrix of eigenvectors corresponding to the original problem as specified by equation (A3) then follows from

$$[X] = [S][Y] \tag{A11}$$

By using the method of Walton and Steeves (ref. 24), a transformation matrix $[\beta]$ is then formed from the columns of $[X]$ corresponding to zero eigenvalues[11] and is used in equation (12) to effect a transformation from dependent coordinates to independent coordinates. For completeness it should be remarked that the computational procedure just described has been numerically verified.

[11]The columns of $[X]$ corresponding to zero eigenvalues will all be grouped at the right in $[X]$ if the Jacobi method is used to solve equation (A9a).

REFERENCES

1. Archer, John S.: A Stiffness Matrix Method of Natural Mode Analysis. National Specialist Meeting, Proceedings, Dynamics and Aeroelasticity (Fort Worth, Texas), Nov. 1958, pp. 88-97.
2. Sciarra, John J.: Dynamic Unified Structural Analysis Method Using Stiffness Matrices. AIAA/ASME Seventh Structures and Materials Conference (Cocoa Beach, Florida), Apr. 1966, pp. 94-112.
3. Zienkeiwicz, O. C.: The Finite Element Method in Structural and Continuum Mechanics. McGraw-Hill Pub. Co. Ltd., c.1967.
4. Hurty, Walter C.; and Rubinstein, Moshe F.: Dynamics of Structures. Prentice-Hall, Inc., c.1964.
5. Przemieniecki, J. S.: Theory of Matrix Structural Analysis. McGraw-Hill Book Co., c.1968.
6. Rubinstein, Moshe F.: Structural Systems – Statics, Dynamics and Stability. Prentice-Hall, Inc., c.1970.
7. Martin, Harold C.; and Carey, Graham F.: Introduction to Finite Element Analysis. McGraw-Hill Book Co., Inc., c.1973.
8. Hurty, Walter C.: Dynamic Analysis of Structural Systems by Component Mode Synthesis. Tech. Rep. No. 32-530 (Contract NAS 7-100), Jet Propulsion Lab., Calif. Inst. Technol., Jan. 1964.
9. Gladwell, G. M. L.: Branch Mode Analysis of Vibrating Systems. J. Sound & Vibration, vol. 1, no. 1, Jan. 1964, pp. 41-59.
10. Goldman, Robert L.: Vibration Analysis by Dynamic Partitioning. RM-305, Martin Co., May 1966.
11. Bamford, R. M.: A Modal Combination Program for Dynamic Analysis of Structures. TM-33-290 (Contract NAS 7-100), Jet Propulsion Lab., Calif. Inst. Technol., Aug. 1966. (Available as NASA CR-82877.)
12. Feng, Chuan C.; and Bajan, Robert L.: Free Vibration Analysis by the Modal Substitution Method. Space Projections From the Rocky Mountain Region; Proceedings of the Symposium (Denver, Colo.), Vol. 2, July 1968.
13. Craig, Roy R., Jr.; and Bampton, Mervyn C. C.: Coupling of Substructures for Dynamic Analysis. AIAA J., vol. 6, July 1968, pp. 1313-1319.
14. Hou, S. N.: Review of Modal Synthesis Techniques and a New Approach. TM-69-2031-5, BellComm, Inc., Sept. 1969. (Available as NASA CR-110769.)

15. Benfield, W. A.; and Hruda, R. F.: Vibration Analysis of Structures by Component Mode Substitution. Paper presented at AIAA/ASME 11th Structures, Structural Dynamics, and Materials Conference (Denver, Colorado), Apr. 1970.

16. Hart, Gary C.; Hurty, Walter C.; and Collins, Jon D.: A Survey of Modal Synthesis Methods. [Preprint] 710783, Soc. Automot. Eng., 1971.

17. Hurty, Walter C.; Collins, Jon D.; and Hart, Gary C.: Dynamic Analysis of Large Structures by Modal Synthesis Techniques. Computers & Structures, vol. 1, nos. 1/2, Aug. 1971, pp. 535-563.

18. MacNeal, Richard H.: A Hybrid Method of Component Mode Synthesis. Computers & Structures, vol. 1, no. 4, Dec. 1971, pp. 581-601.

19. Benfield, W. A.; Bodley, C. S.; and Morosow, G.: Modal Synthesis Methods. Paper presented at Symposium on Substructure Testing and Synthesis (Marshall Space Flight Center), Aug. 30, 1972.

20. Dowell, E. H.: Free Vibrations of an Arbitrary Structure in Terms of Component Modes. Trans. ASME, Ser. E: J. Appl. Mech., vol. 39, no. 3, Sept. 1972, pp. 727-732.

21. Kuhar, E. J.; and Stahle, C. V.: A Dynamic Transformation Method for Modal Synthesis. AIAA Paper No. 73-396, Mar. 1973.

22. Wada, B. K.; Garba, J. A.; and Chen, J. C.: Development and Correlation: Viking Orbiter Analytical Dynamic Model With Modal Test. Tech. Memo. 33-690, Jet Propulsion Lab., Calif. Inst. Technol., June 1974. (Available as NASA CR-138728.)

23. Rubin, S.: An Improved Component-Mode Representation. AIAA Paper No. 74-386, Apr. 1974.

24. Walton, William C., Jr.; and Steeves, Earl C.: A Practical Computational Method for Reducing a Dynamical System With Constraints to an Equivalent System With Independent Coordinates. Paper presented at Air Force Second Conference on Matrix Methods in Structural Mechanics (Wright-Patterson Air Force Base, Ohio), Oct. 15-17, 1968.

25. Walton, William C., Jr.; and Steeves, Earl C.: A New Matrix Theorem and Its Application for Establishing Independent Coordinates for Complex Dynamical Systems With Constraints. NASA TR R-326, 1969.

26. Greene, B. E.; Jones, R. E.; McLay, R. W.; and Strome, D. R.: Generalized Variational Principles in the Finite-Element Method. AIAA J., vol. 7, no. 7, July 1969, pp. 1254-1260.

27. Gauzy, H.: Measurement of Inertia and Structural Damping. AGARD Manual on Aeroelasticity, Part IV, Chapter 3, Oct. 1968.

28. Marcus, Marvin: Basic Theorems in Matrix Theory. Nat. Bur. Stand., Appl. Math. Ser. 57, U.S. Dept. Com., Jan. 22, 1960. (Reprinted 1964.)

29. Wilkinson, J. H.; and Reinsch, C.: Handbook for Automatic Computation. Volume II – Linear Algebra, Springer-Verlag, 1971.

30. Wilkinson, J. H.: The Algebraic Eigenvalue Problem. Clarendon Press (Oxford), c.1965.

31. Ralston, Anthony: A First Course in Numerical Analysis. McGraw-Hill Book Co., Inc., c.1965.

32. White, Paul A.: The Computation of Eigenvalues and Eigenvectors of a Matrix. J. Soc. Ind. Appl. Math., vol. 6, no. 4, Dec. 1958, pp. 393-437.

33. Bishop, R. E. D.; Gladwell, G. M. L.; and Michaelson, S.: The Matrix Analysis of Vibration. Cambridge Univ. Press, 1965.

34. Ortega, James: The Givens-Householder Method for Symmetric Matrices. Mathematical Methods for Digital Computers, Vol. II, Anthony Ralston and Herbert S. Wilf, eds., John Wiley & Sons, Inc., c.1967, pp. 94-115.

35. Bathe, Klaus-Jürgen; and Wilson, Edward L.: Solution Methods for Eigenvalue Problems in Structural Mechanics. Internat. J. for Numerical Methods in Engineering, vol. 6, no. 2, 1973, pp. 213-226.

36. Walton, William C., Jr.: Applications of a General Finite-Difference Method for Calculating Bending Deformations of Solid Plates. NASA TN D-536, 1960.

37. Guyan, Robert J.: Reduction of Stiffness and Mass Matrices. AIAA J., vol. 3, no. 2, Feb. 1965, p. 380.

38. Peters, G.; and Wilkinson, J. H.: $Ax = \lambda Bx$ and the Generalized Eigenproblem. SIAM J. Numer. Anal., vol. 7, no. 4, Dec. 1970, pp. 479-492.

39. Moler, C. B.; and Stewart, G. W.: An Algorithm for Generalized Matrix Eigenvalue Problems. SIAM J. Numerical Anal., vol. 10, no. 2, Apr. 1973, pp. 241-256.

40. Dettman, John W.: Mathematical Methods in Physics and Engineering. McGraw-Hill Book Co., Inc., 1962.

41. Meirovitch, Leonard: Analytical Methods in Vibrations. Macmillan Co., c.1967.

42. Fralich, Robert W.; Green, Claude E.; and Rheinfurth, Mario H.: Dynamic Analysis for Shuttle Design Verification. NASA Space Shuttle Technology Conference, Dynamics and Aeroelasticity; Structures and Materials, NASA TM X-2570, pp. 205-230.

43. Thornton, E. A.: Vibration Analysis of a 1/15 Scale Dynamic Model of a Space Shuttle Configuration. Grant No. NAS1-9434-20, Old Dominion Univ., [1972]. (Available as NASA CR-111984.)

44. Williams, Edward H.: Design Control Specification for a One-Thirtieth Scale B-52E Flexible Model. Doc. No. D3-7387-1, Boeing Co., June 15, 1967.

45. Redd, L. T.; Gilman, J., Jr.; Cooley, D. E.; and Sevart, F. D.: A Wind-Tunnel Investigation of a B-52 Model Flutter Suppression System. AIAA Paper No. 74-401, Apr. 1974.

TABLE I.- DISCRETIZATION EMPLOYED FOR FREE-FREE UNIFORM BEAM

(a) Direct analysis of complete beam

20 Degrees of Freedom (D.O.F.)

Station	Local coordinate position, cm	Mass, kg	Rotary inertia, kg-cm^2	EI, kN-cm^2
1	0.00	0.74	153.66	1434.9
2	15.24	1.48	306.19	
3	30.48			
4	45.72			
5	60.96			
6	76.20			
7	91.44			
8	106.68			
9	121.92	1.48	306.19	1434.9
10	137.16	.74	153.66	—

(b) Component-mode synthesis analysis of beam

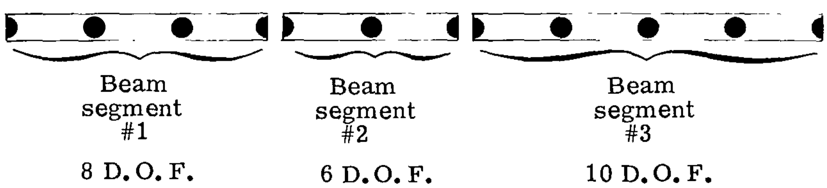

Station	Local coordinate position, cm	Mass, kg	Rotary inertia, kg-cm^2	EI, kN-cm^2
Beam 1				
1	0.00	0.74	153.66	1434.9
2	15.24	1.48	306.19	1434.9
3	30.48	1.48	306.19	1434.9
4	45.72	.74	153.09	—
Beam 2				
1	0.00	.74	153.09	1434.9
2	15.24	1.48	306.19	1434.9
3	30.48	.74	153.09	—
Beam 3				
1	0.0	.74	153.09	1434.9
2	15.24	1.48	306.19	1434.9
3	30.48	1.48	306.19	1434.9
4	45.72	1.48	306.19	1434.9
5	60.96	.74	153.66	—

TABLE II.- COMPARISON OF CALCULATED FREQUENCIES (Hz)

FOR FREE-FREE UNIFORM BEAM

Mode	Direct solution	Modal synthesis				
		Full	Partial	Partial	Partial	Partial
		a(8,6,10)	a(6,5,7)	a(4,4,4)	a(4,3,5)	a(3,3,3)
1	0	0	0	0	0	0
2	0	0	0	0	0	0
3	5.7016	5.7016	5.7171	5.9313	5.8135	6.3517
4	13.0848	13.0848	13.0890	13.3037	13.5910	14.0724
5	21.7817	21.7817	21.8156	22.2553	22.2265	23.2227
6	30.7180	30.7180	30.7484	31.4144	32.0870	-------
7	39.0547	39.0547	39.0888	40.0870	41.4177	-------
8	46.1034	46.1034	46.1238	49.5418	42.2940	-------
9	51.4069	51.4069	51.4181	-------	-------	-------
10	54.6867	54.6867	54.6937	-------	-------	-------

[a]Numbers in parentheses indicate the number of lowest component modes (rigid body and elastic) selected from each of the three beam segments for use in the synthesizing procedure.

TABLE III.- COMPARISON OF CALCULATED MODE SHAPES FOR

FREE-FREE UNIFORM BEAM FOURTH ELASTIC MODE

		Direct solution	Full coupling a(8, 6, 10)	Partial coupling a(6, 5, 7)	Partial coupling a(4, 3, 5)
Beam segment 1	Displacements	1.5407849E+00	1.5407849E+00	1.5277206E+00	1.0720708E+00
		-2.1099470E+00	-2.1099470E+00	-2.1057819E+00	-1.6459134E+00
		-8.6324372E-01	-8.6324372E-01	-7.9926286E-01	-4.8519823E-01
		2.4186786E+00	2.4186786E+00	2.3858377E+00	1.7102538E+00
	Slopes	-9.1589550E-01	-9.1589550E-01	-9.1854928E-01	-7.9281501E-01
		-2.7198374E-01	-2.7198374E-01	-2.7269507E-01	-8.8633943E-02
		6.3707187E-01	6.3707187E-01	6.4296516E-01	4.4316537E-01
		3.7389223E-01	3.7389223E-01	3.8383215E-01	2.7372653E-01
Beam segment 2	Displacements	2.4186786E+00	2.4186786E+00	2.3858377E+00	1.7102538E+00
		1.8153843E+00	1.8153843E+00	1.7831773E+00	1.8284178E+00
		-1.8153843E+00	-1.8153843E+00	-1.7970272E+00	-1.3720709E+00
	Slopes	3.7389223E-01	3.7389223E-01	3.8383215E-01	2.7372653E-01
		-5.6685512E-01	-5.6685512E-01	-5.6202334E-01	-2.5686039E-01
		-5.6685512E-01	-5.6685512E-01	-5.6826866E-01	-7.8744731E-01
Beam segment 3	Displacements	-1.8153843E+00	-1.8153843E+00	-1.7970272E+00	-1.3720709E+00
		-2.4186786E+00	-2.4186786E+00	-2.4279521E+00	-3.0063475E+00
		8.6324372E-01	8.6324372E-01	8.5461047E-01	7.0630864E-01
		2.1099470E+00	2.1099470E+00	2.1110319E+00	2.5721887E+00
		-1.5407849E+00	-1.5407849E+00	-1.5369871E+00	-1.6873487E+00
	Slopes	-5.6685512E-01	-5.6685512E-01	-5.6826866E-01	-7.8744731E-01
		3.7389223E-01	3.7389223E-01	3.7240325E-01	2.6499591E-01
		6.3707187E-01	6.3707187E-01	6.3816020E-01	8.7039310E-01
		-2.7198374E-01	-2.7198374E-01	-2.7114062E-01	-3.2056058E-01
		-9.1589550E-01	-9.1589550E-01	-9.1620300E-01	-1.0648398E+00

[a]Numbers in parentheses indicate the number of lowest component modes (rigid body and elastic) selected from each of the three beam segments for use in the synthesizing procedure.

TABLE IV.- DISCRETIZATION EMPLOYED FOR

AIRPLANE BEAM ASSEMBLY

Station	Local coordinate position, cm	Mass,[a] kg	Torsional inertia, kg-cm^2	EI, kN-cm^2	GJ, kN-cm^2
			Fuselage		
1	0.00	0.03648	Not applicable	1371.5	Not applicable
2	10.16	.07296			
3	20.32	.07296			
4	30.48	.07296			
5	40.64	.06567			
[b]6	48.77	.52653			
7	60.96	.08026			
8	71.12	.07296			
9	81.28	.07296			
10	91.44	.07296			
11	101.60	.06567			
12	109.73	.07296			
13	121.92	.04378		------	
			Wing		
1	0.00	0.06487	0.1395	270.91	451.13
2	10.16	.12975	.2790		
3	20.32				
4	30.48				
5	40.64				
6	50.80				
7	60.96	.06487	.1395	------	------
			Horizontal tail		
1	0.00	0.03243	0.06979	270.91	451.13
2	5.08	.06487	.13958		
3	10.16				
4	15.24				
5	20.32				
6	25.40	.03243	.06979	------	------

[a]Rotary inertia of lumped masses neglected.

[b]Mass of shaker stem and coil included.

TABLE V.- COMPARISON OF CALCULATED AND MEASURED SYMMETRIC MODE FREQUENCIES (Hz) FOR AIRPLANE BEAM ASSEMBLY

Mode	Direct solution	Full modal synthesis		Partial modal synthesis			Measured
		Free-free fuselage, wing and tail modes		Free-free fuselage modes			
			Quasi-component modes	Clamped-free wing and tail modes	Pinned-free wing and tail modes	Free-free wing and tail modes	
1	0	0	0	0	0	0	-----
2	0	0	0	0	0	0	-----
3	7.3769	8.0234	7.3769	7.4157	8.2024	8.3214	8.0
4	21.4885	21.5986	21.4885	21.5053	21.6805	21.7254	21.5
5	45.9255	50.8958	45.9255	46.2597	53.2747	54.2784	50.9
6	51.8871	54.9862	51.8871	52.3714	57.9148	59.7710	55.2
7	84.3666	86.8019	84.3666	85.0963	90.5896	94.9088	88.4
8	115.6038	127.8944	115.6038	116.4056	133.1559	134.2964	128.4
9	151.8068	154.3213	151.8068	153.3172	159.3065	160.3770	162.2
10	174.2613	175.4510	174.2613	177.1566	184.0957	184.1293	-----

TABLE VI.- COMPARISON OF CALCULATED SYMMETRIC MODE SHAPES

FOR AIRPLANE BEAM ASSEMBLY (FOURTH ELASTIC MODE)

		Direct solution	Full modal synthesis		Partial modal synthesis		
			Free-free fuselage, wing, and tail modes		Free-free fuselage modes		
				Quasi-component modes	Clamped-free wing and tail modes	Pinned-free wing and tail modes	Free-free wing and tail modes
Fuselage	Displacements	1.6521193E+01	1.7304901E+01	1.6521193E+01	1.6594463E+01	1.7608114E+01	1.7819170E+01
		8.9877509E+00	9.1300295E+00	8.9877509E+00	9.0384015E+00	9.1448802E+00	9.0999976E+00
		2.0329730E+00	1.6326853E+00	2.0329730E+00	1.9812090E+00	1.3547642E+00	1.1355911E+00
		-3.3890805E+00	-4.0861526E+00	-3.3890804E+00	-3.5027696E+00	-4.4415989E+00	-4.7009078E+00
		-5.1886494E+00	-6.7970397E+00	-6.1886494E+00	-6.2011387E+00	-6.7896369E+00	-6.9039300E+00
		-5.9109087E+00	-6.1161571E+00	-5.9109087E+00	-5.8859563E+00	-5.6004908E+00	-5.3778789E+00
		-1.8465204E+00	-1.3389632E+00	-1.8465204E+00	-1.6779757E+00	7.2080836E-01	1.8829467E+00
		3.0643879E+00	3.8656010E+00	3.0643879E+00	3.4702656E+00	7.4780252E+00	9.4649418E+00
		7.7670079E+00	8.4619894E+00	7.7670078E+00	8.2944168E+00	1.2886464E+01	1.5274581E+01
		1.0942433E+01	1.1085374E+01	1.0942433E+01	1.1361834E+01	1.4987303E+01	1.7035672E+01
		1.1717232E+01	1.0912538E+01	1.1717231E+01	1.1875342E+01	1.2939452E+01	1.3872282E+01
		1.0412129E+01	8.6515348E+00	1.0412129E+01	1.0560546E+01	8.7025131E+00	8.3343843E+00
		7.3731216E+00	4.0351336E+00	7.3731216E+00	6.9485543E+00	-7.2870064E-03	-2.6414825E+00
	Slopes	-1.9037704E+00	-2.0675509E+00	-1.9037704E+00	-1.9041170E+00	-2.1373948E+00	-2.2050479E+00
		-1.8425407E+00	-1.9960515E+00	-1.8425407E+00	-1.8588122E+00	-2.0726358E+00	-2.1292837E+00
		-1.5922319E+00	-1.7024047E+00	-1.5922319E+00	-1.6205747E+00	-1.7620743E+00	-1.7905018E+00
		-1.0711554E+00	-1.1064665E+00	-1.0711554E+00	-1.0647673E+00	-1.0693263E+00	-1.0593881E+00
		-2.8936322E-01	-1.9402322E-01	-2.8936322E-01	-2.5711691E-01	-7.0521396E-02	-1.5865870E-03
		4.7927251E-01	5.9545194E-01	4.7927251E-01	4.5389674E-01	8.1501981E-01	9.6208181E-01
		1.1286242E+00	1.2570124E+00	1.1286242E+00	1.1894047E+00	1.6537318E+00	1.8759962E+00
		1.2623677E+00	1.2862834E+00	1.2623677E+00	1.3134395E+00	1.6173894E+00	1.7877887E+00
		1.0320514E+00	9.4854450E-01	1.0320514E+00	1.0361316E+00	1.0009521E+00	1.0165751E+00
		5.1796050E-01	3.3436225E-01	5.1796050E-01	4.6071046E-01	1.0760351E-02	-1.7604115E-01
		-1.4122561E-01	-4.4808212E-01	-1.4122560E-01	-1.9327917E-01	-1.0042526E+00	-1.3641350E+00
		-6.6461082E-01	-8.7778524E-01	-6.6461081E-01	-5.9728038E-01	-1.5941397E+00	-2.0380944E+00
		-6.1738434E-01	-1.0037323E+00	-6.1738433E-01	-8.3010708E-01	-1.9247427E+00	-2.4109112E+00
		0.	0.	0.	0.	0.	0.
Wing	Displacements	-5.9109087E+00	-6.1161571E+00	-5.9109087E+00	-5.8859563E+00	-5.6004908E+00	-5.3778789E+00
		-2.8247060E+00	-3.8420516E+00	-2.8247060E+00	-2.7948218E+00	-3.4835066E+00	-3.2000837E+00
		2.3852848E+00	2.3848040E+00	2.3852849E+00	2.2036757E+00	5.8102183E-01	-1.4108857E-02
		5.8543199E+00	7.1491205E+00	5.8543200E+00	5.5617852E+00	4.3482246E+00	2.8527983E+00
		4.8362076E+00	6.3193019E+00	4.8362077E+00	4.7284910E+00	4.1780357E+00	2.9312190E+00
		-6.8898880E-01	-5.0890464E-01	-6.8898885E-01	-5.7401759E-01	-2.6747499E-01	-1.2224710E-01
		-8.5602782E+00	-1.0550333E+01	-8.5602784E+00	-8.3513136E+00	-6.6263127E+00	-4.6237932E+00
	Slopes	2.3963676E-01	2.9772660E-01	2.3963676E-01	2.2694885E-01	4.0751077E-01	4.8104192E-01
		1.1859534E+00	1.1101259E+00	1.1859534E+00	1.1649864E+00	7.7271660E-01	6.7126259E-01
		1.2386949E+00	1.6374906E+00	1.2386949E+00	1.1803297E+00	1.1377573E+00	8.5673527E-01
		3.6853644E-01	5.6325077E-01	3.6853645E-01	3.8115005E-01	5.5005268E-01	4.4145778E-01
		-8.7464862E-01	-1.0197802E+00	-8.7464864E-01	-8.1131846E-01	-6.4020758E-01	-4.1357054E-01
		-1.7774235E+00	-2.2476087E+00	-1.7774235E+00	-1.7377283E+00	-1.4509970E+00	-1.0164597E+00
		-2.0630218E+00	-2.6416914E+00	-2.0630218E+00	-2.0476219E+00	-1.6590656E+00	-1.1788500E+00
	Twists	-4.1506188E-01	-5.1567614E-01	-4.1506188E-01	-3.9308583E-01	-7.0582736E-01	-8.3318670E-01
		-4.3177798E-01	-5.3928184E-01	-4.3177798E-01	-4.0868902E-01	-7.1886811E-01	-8.4970222E-01
		-4.4560976E-01	-5.5884190E-01	-4.4560976E-01	-4.2254842E-01	-7.4977819E-01	-8.8885313E-01
		-4.5646482E-01	-5.7420957E-01	-4.5646482E-01	-4.3343765E-01	-7.8083951E-01	-9.2820830E-01
		-4.6427065E-01	-5.8526958E-01	-4.6427064E-01	-4.4089650E-01	-7.9901132E-01	-9.5125223E-01
		-4.6897510E-01	-5.9193895E-01	-4.6897510E-01	-4.4509713E-01	-8.0414238E-01	-9.5778063E-01
		-4.7054675E-01	-5.9416764E-01	-4.7054675E-01	-4.4643375E-01	-8.0429361E-01	-9.5798490E-01
		0.	0.	0.	0.	0.	0.
Tail	Displacements	1.0412129E+01	8.6515348E+00	1.0412129E+01	1.0560546E+01	8.7025131E+00	8.3343843E+00
		8.0946739E+00	7.1294468E+00	8.0946739E+00	8.1211910E+00	6.7763950E+00	6.0861761E+00
		2.8958563E+00	2.7226646E+00	2.8958563E+00	2.7227309E+00	3.0311565E+00	2.5528668E+00
		-4.3742001E+00	-3.7629538E+00	-4.3742001E+00	-4.5888876E+00	-3.4201934E+00	-3.4138671E+00
		-1.2820274E+01	-1.1432520E+01	-1.2820274E+01	-1.2900508E+01	-1.2172483E+01	-1.1814026E+01
		-2.1699619E+01	-1.9539528E+01	-2.1699619E+01	-2.1556928E+01	-2.2024800E+01	-2.1499285E+01
	Slopes	-3.3230612E-01	-4.3889405E-01	-3.3230611E-01	-2.9864082E-01	-7.9707155E-01	-1.0190493E+00
		-1.9377348E+00	-1.4053439E+00	-1.9377348E+00	-2.0493517E+00	-1.2950342E+00	-1.3342136E+00
		-3.1911635E+00	-2.8330356E+00	-3.1911634E+00	-3.2606742E+00	-2.5298267E+00	-2.3163724E+00
		-4.0009223E+00	-3.6011145E+00	-4.0009223E+00	-3.9730693E+00	-3.8805417E+00	-3.6503615E+00
		-4.3793420E+00	-3.9952829E+00	-4.3793420E+00	-4.2819077E+00	-4.7534658E+00	-4.6325203E+00
		-4.4698381E+00	-4.0826143E+00	-4.4698381E+00	-4.3513611E+00	-5.0125048E+00	-4.9476846E+00
	Twists	5.7556945E-01	7.6013464E-01	5.7556944E-01	5.1725962E-01	1.3805645E+00	1.7650402E+00
		5.7996372E-01	7.6671491E-01	5.7996371E-01	5.2083097E-01	1.3834856E+00	1.7690223E+00
		5.8338912E-01	7.7180676E-01	5.8338911E-01	5.2405274E-01	1.3911330E+00	1.7794475E+00
		5.8583993E-01	7.7545063E-01	5.8583992E-01	5.2660955E-01	1.4005857E+00	1.7923337E+00
		5.8731206E-01	7.7763969E-01	5.8731205E-01	5.2825123E-01	1.4087331E+00	1.8027589E+00
		5.8780304E-01	7.7636984E-01	5.8780303E-01	5.2881677E-01	1.4111542E+00	1.8067409E+00
		0.	0.	0.	0.	0.	0.

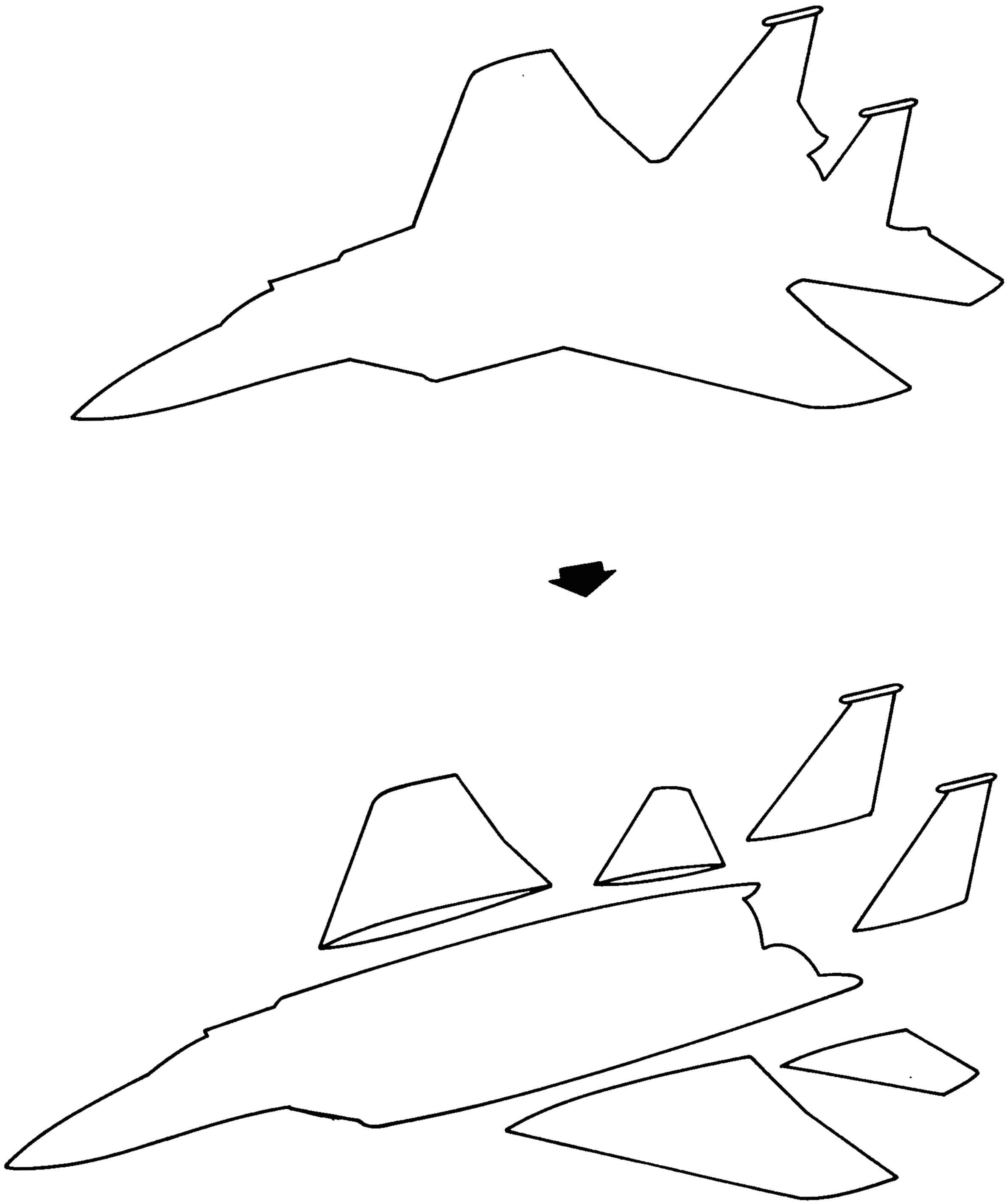

Figure 1.- Partitioning an aircraft structure into several smaller substructures.

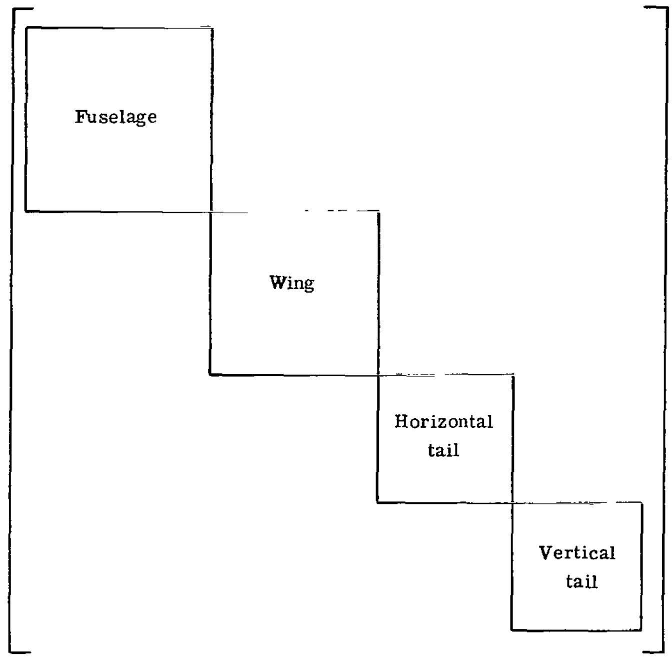

Figure 2.- Block diagonal composition of uncoupled system mass and stiffness matrices ($[\overline{M}]$ and $[\overline{K}]$) for aircraft of figure 1.

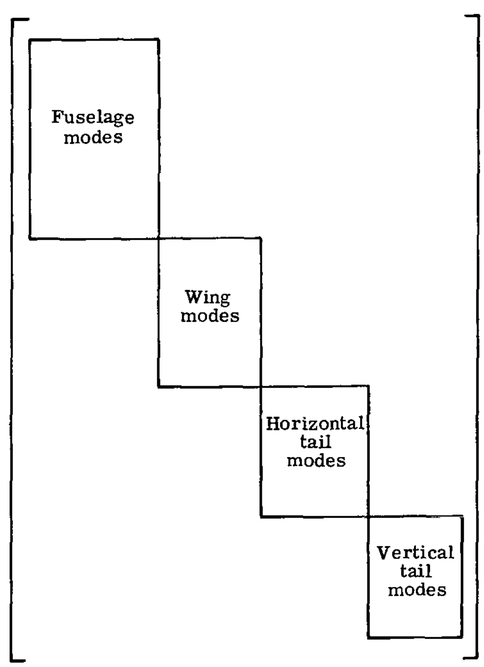

Figure 3.- Block diagonal composition of uncoupled system modal expansion matrix $[U]$ for aircraft of figure 1.

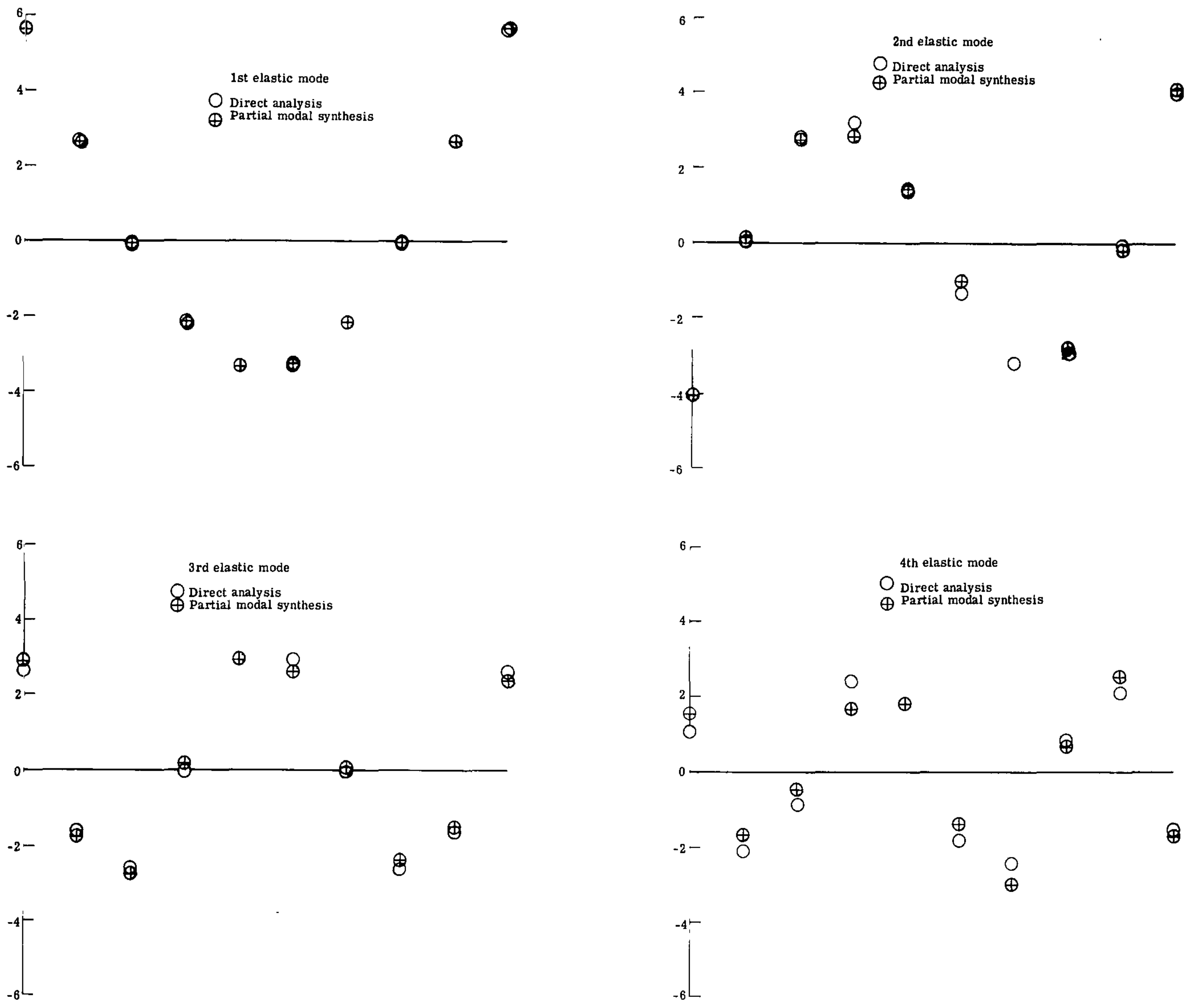

Figure 4.- Comparison of calculated elastic mode shapes for free-free beam. Partial modal synthesis results correspond to case denoted by (4,3,5) in table II.

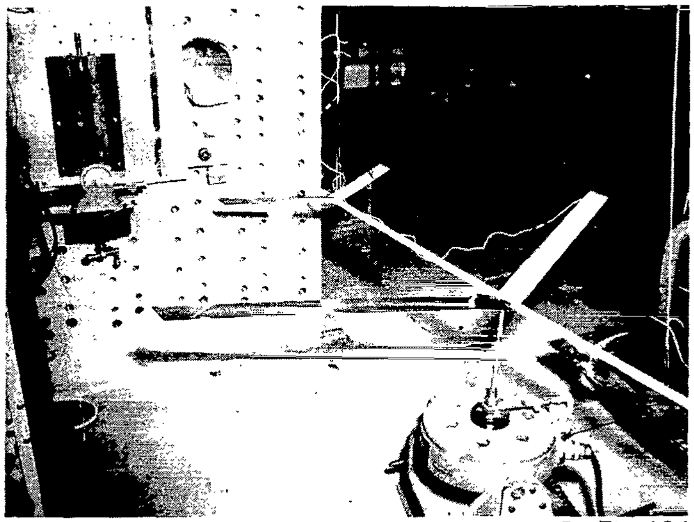

L-75-184

Figure 5.- Airplane beam model during shake test.

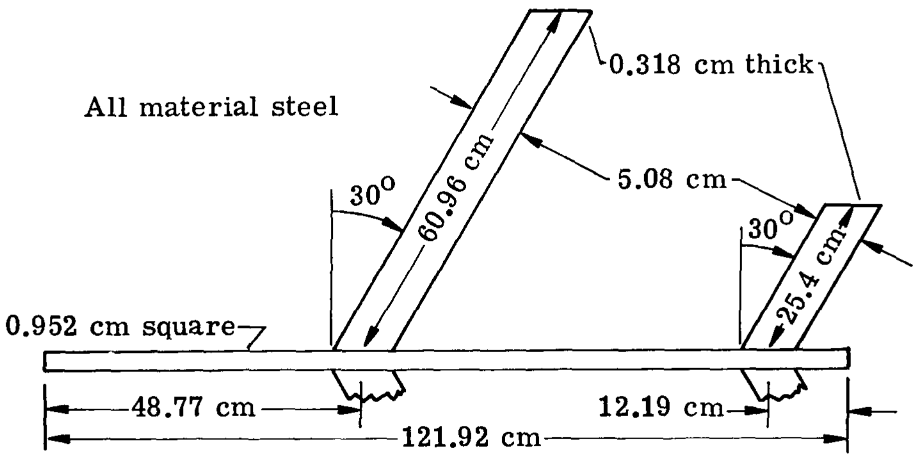

Figure 6.- Geometric properties of airplane beam model.

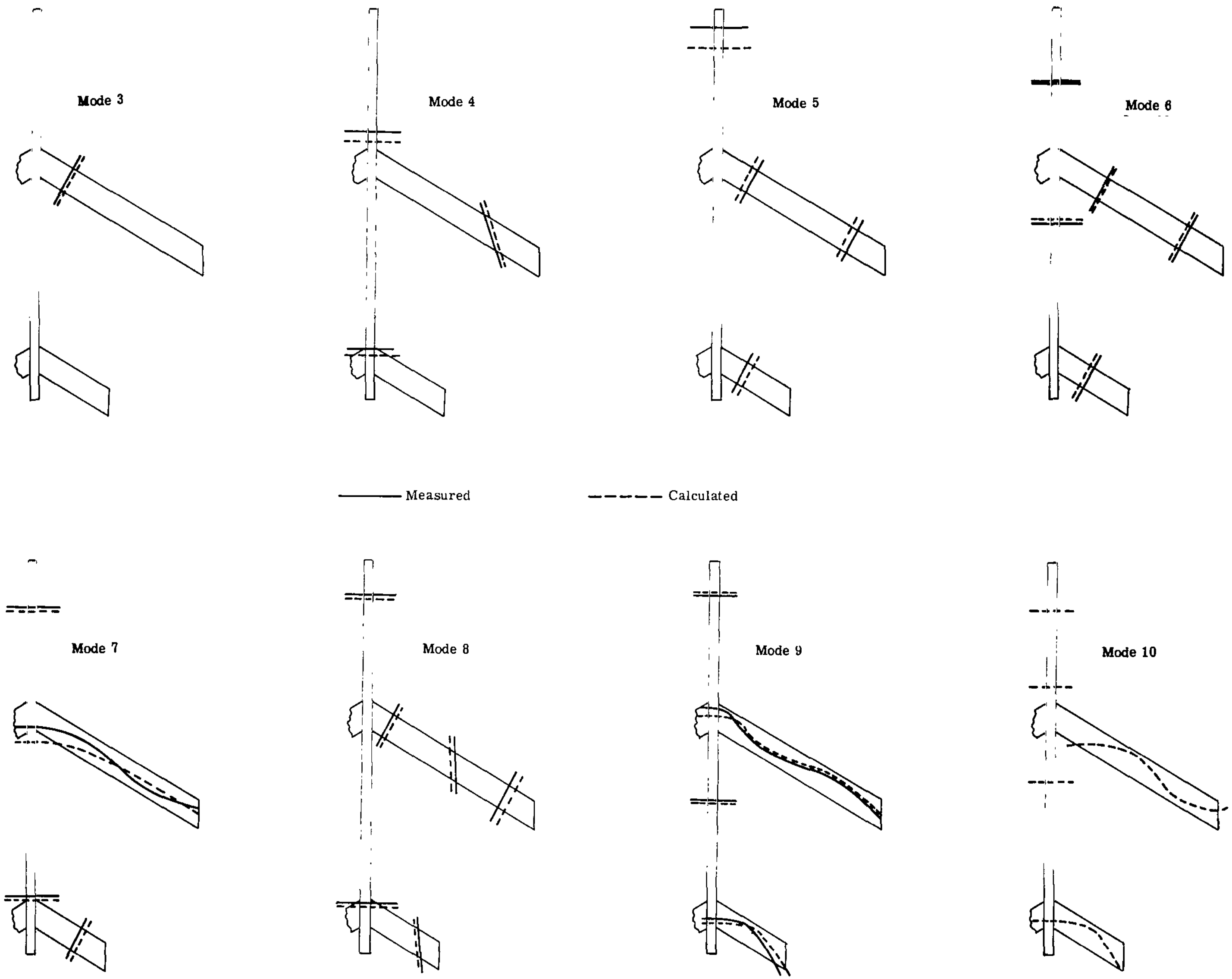

Figure 7.- Comparison of measured and calculated node lines for symmetric elastic modes of airplane beam model. Calculated results are from a direct analysis. Since the experimental node lines are symmetric about the vertical plane of symmetry, the results for only half of the model are shown.

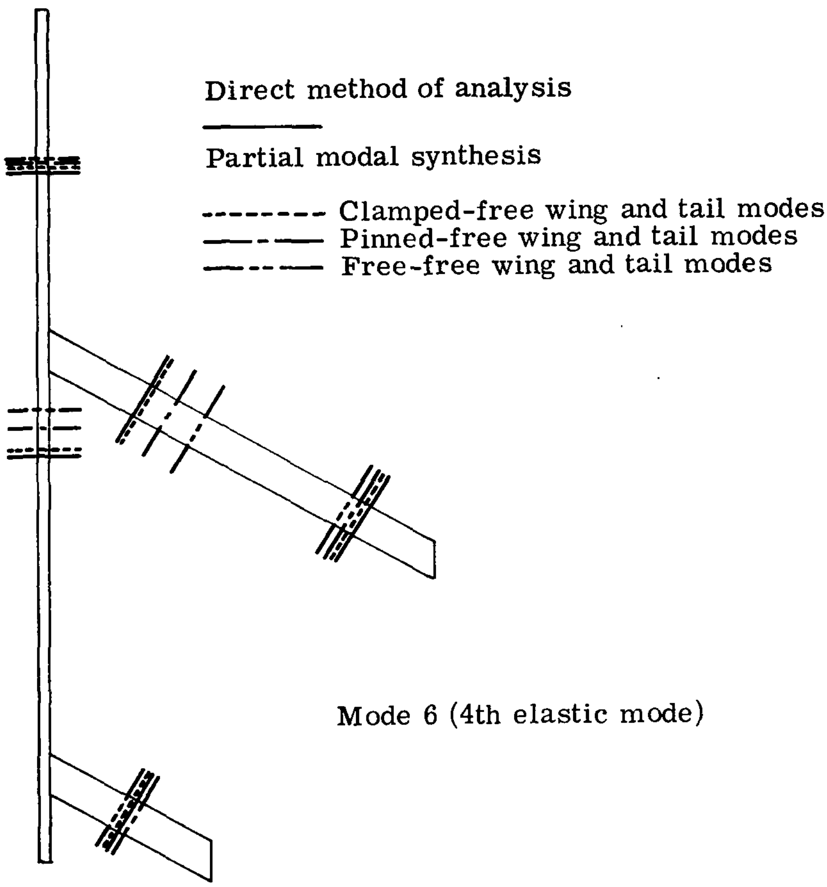

Figure 8.- Comparison of calculated node lines for mode 6 (4th elastic mode) of airplane beam assembly.

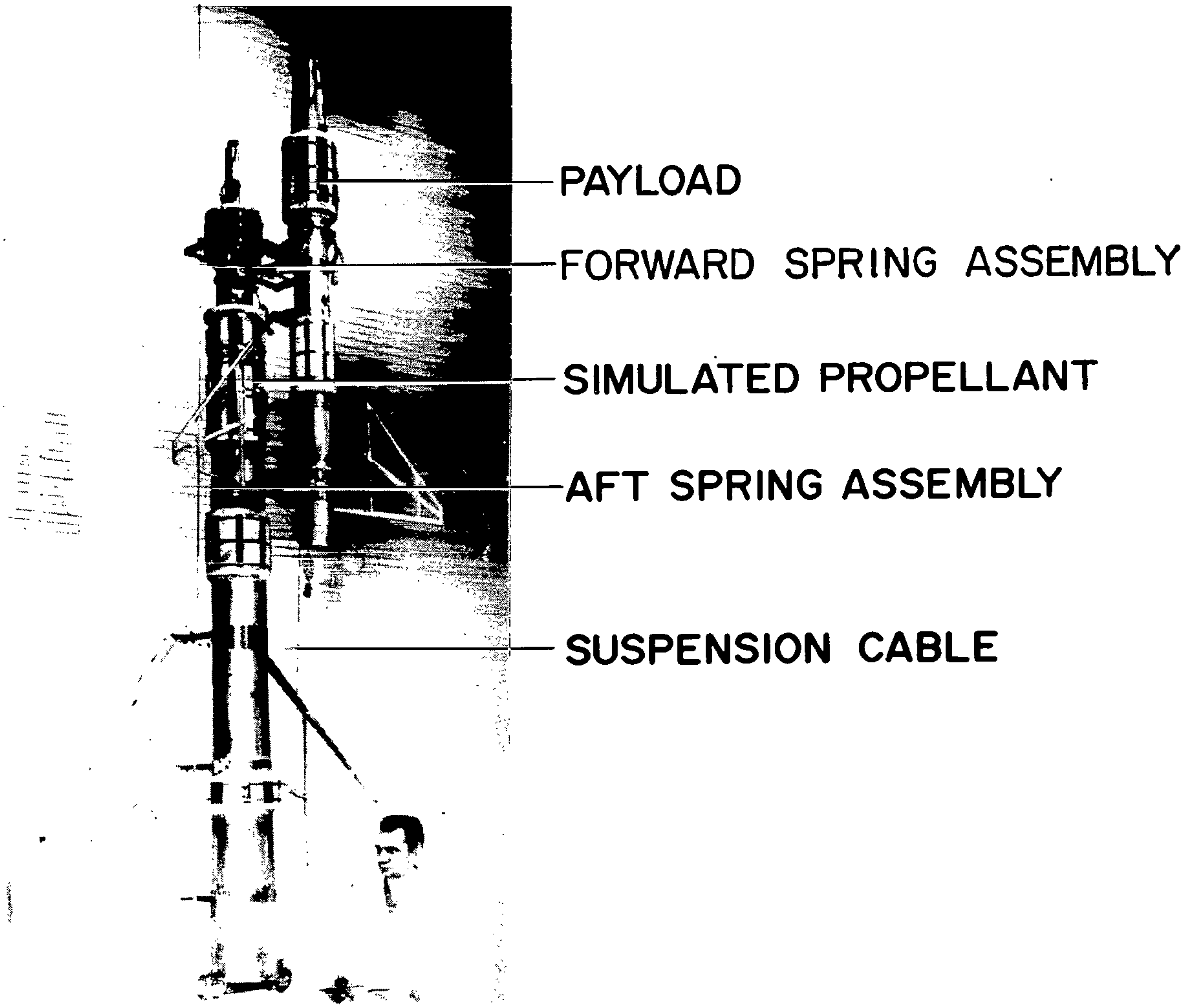

Figure 9.- A 1/15-scale dynamic model of early space shuttle concept.

MODE	FREQUENCIES, Hz			
	EXPERIMENTAL	INTERFACE		
		PINNED	FIXED	FLEXIBLE
1	11.1	10.4	11.2	11.0
2	26.5	29.4	24.9	26.6
3	38.1	40.0	37.4	37.8
4	48.3	----	75.2	48.3
5	98.3	103.5	104.9	100.0
6	101.9	101.5	118.7	113.2

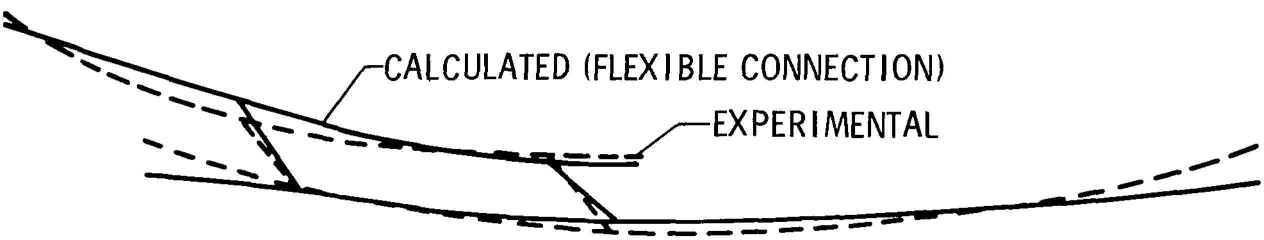

FOURTH MODE SHAPE

Figure 10.- Comparison of experimental and calculated frequencies for 1/15-scale space shuttle dynamic model (reproduced from ref. 42).

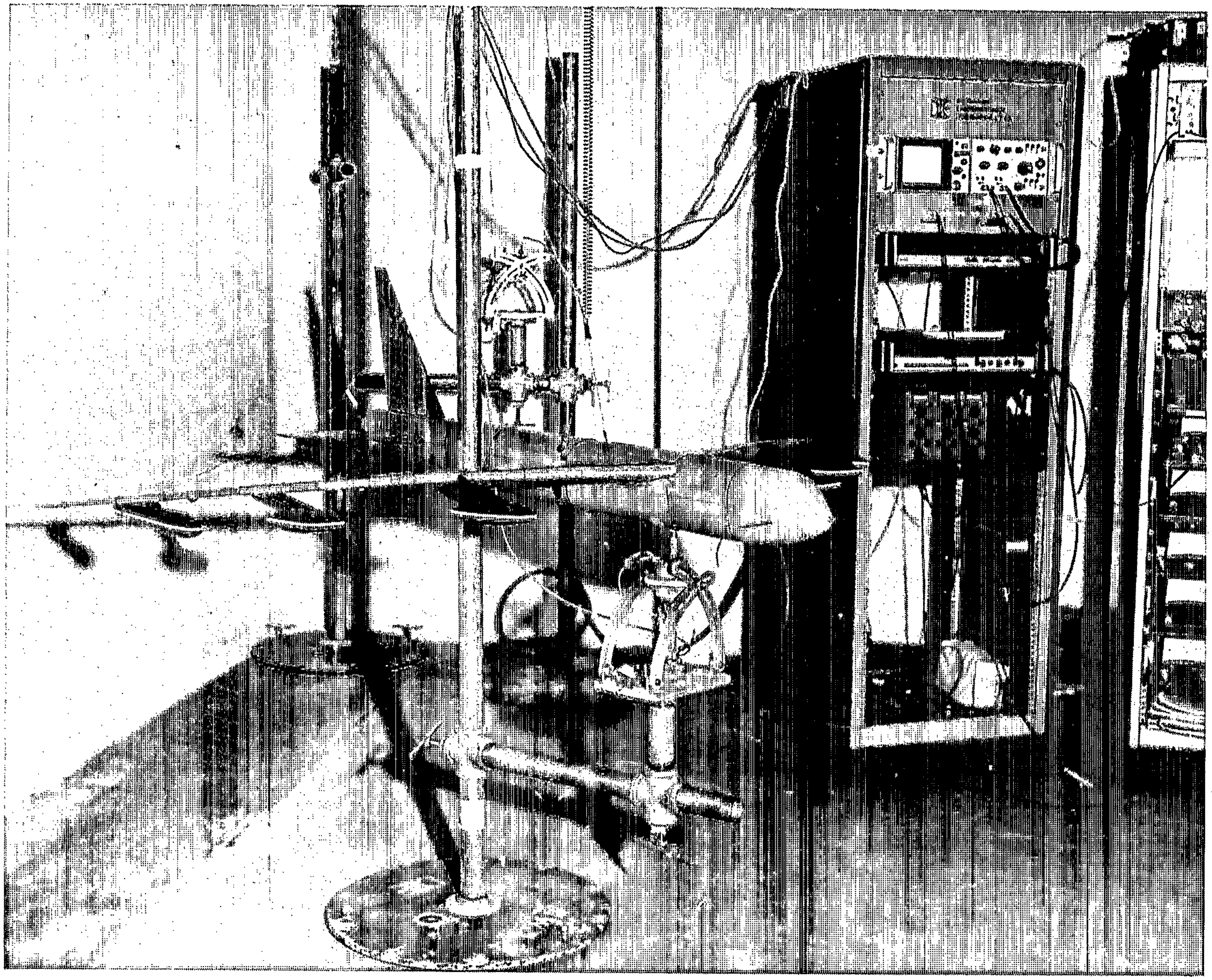

L-74-4930

Figure 11.- A 1/30-scale dynamic aeroelastic model of B-52E airplane.

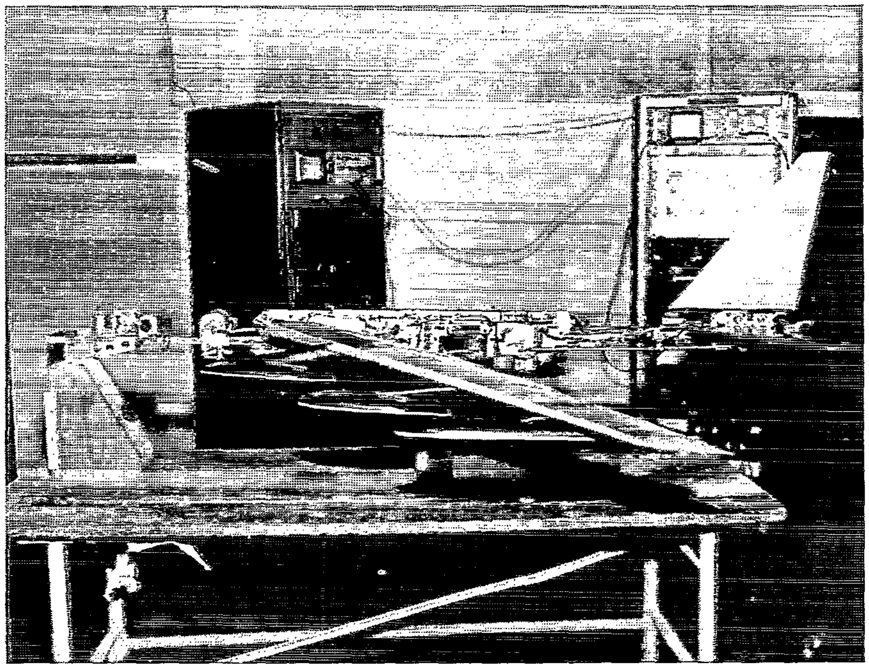

L-74-4934

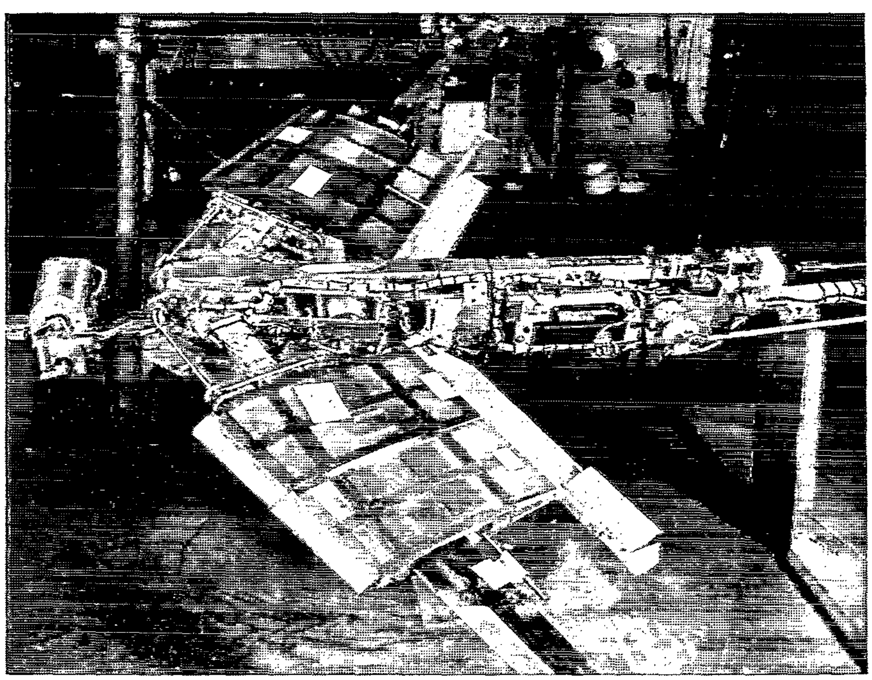

L-73-2151

Figure 12.- A 1/30-scale model of B-52E with several of the segmented shell structures forming the external aerodynamic shape removed.

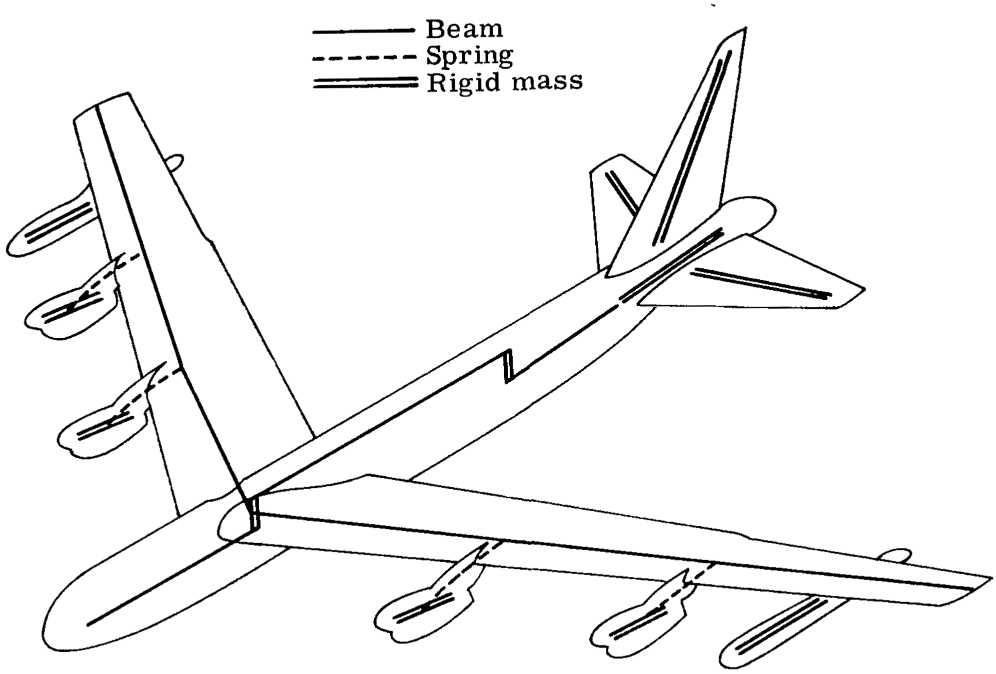

Figure 13.- Beam representation employed for symmetric vibration analysis of 1/30-scale model of B-52E airplane.

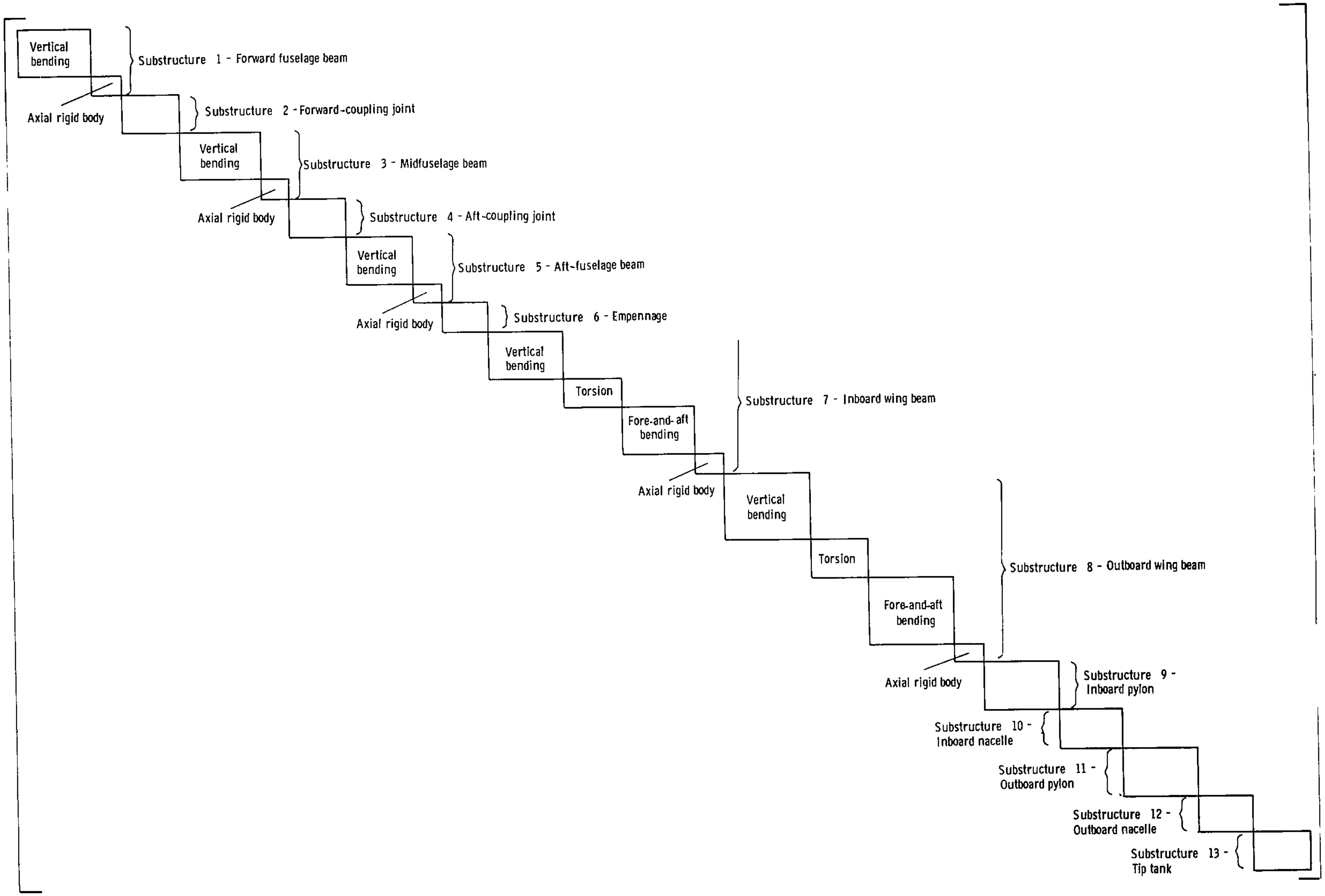

Figure 14.- Block diagonal composition of uncoupled system mass and stiffness matrices ($[\overline{M}]$ and $[\overline{K}]$) corresponding to the beam representation of the 1/30-scale model of the B-52E given in figure 13.

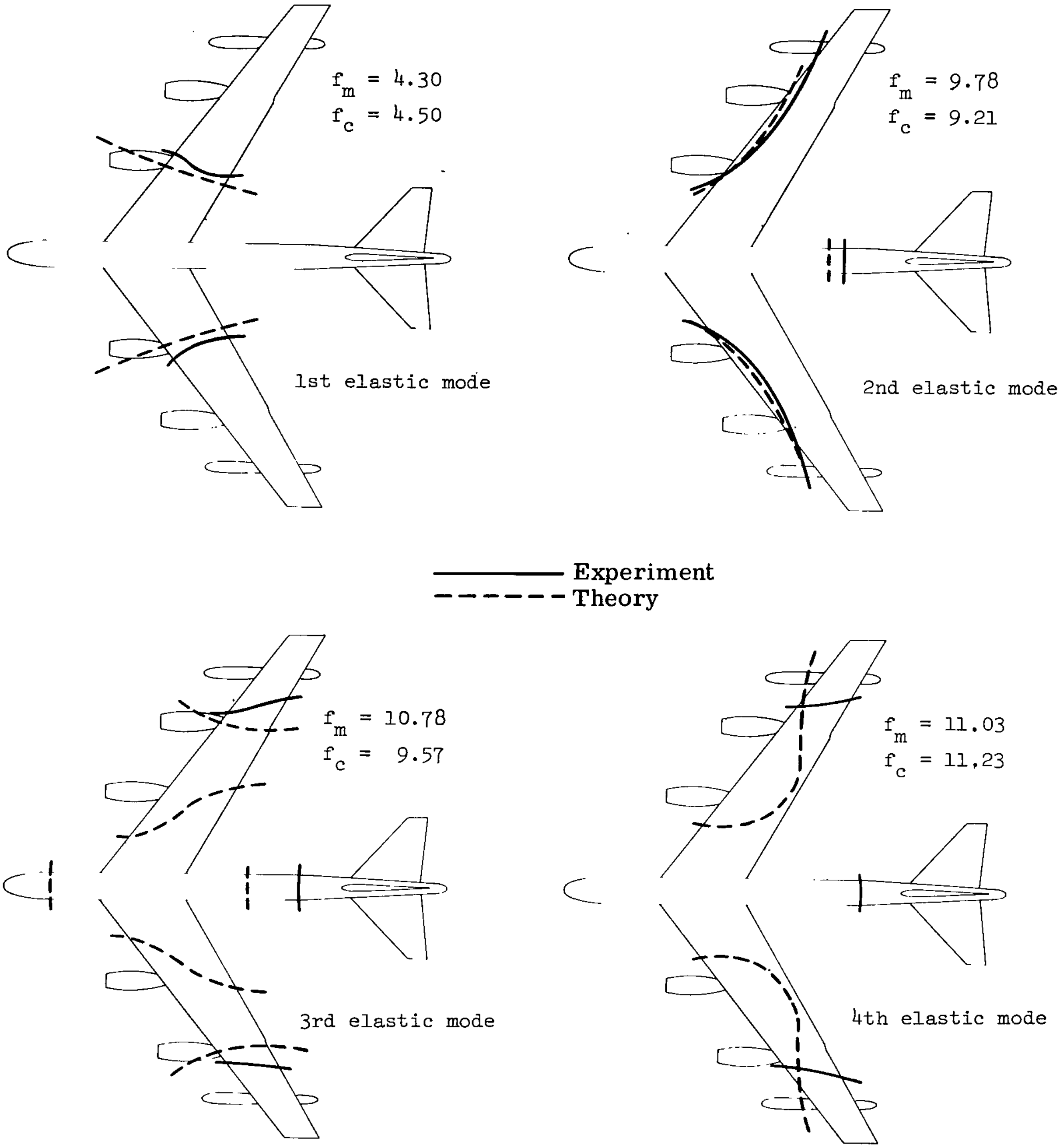

Figure 15.- Comparison of measured and calculated elastic mode frequencies and node lines for 1/30-scale model of B-52E airplane.

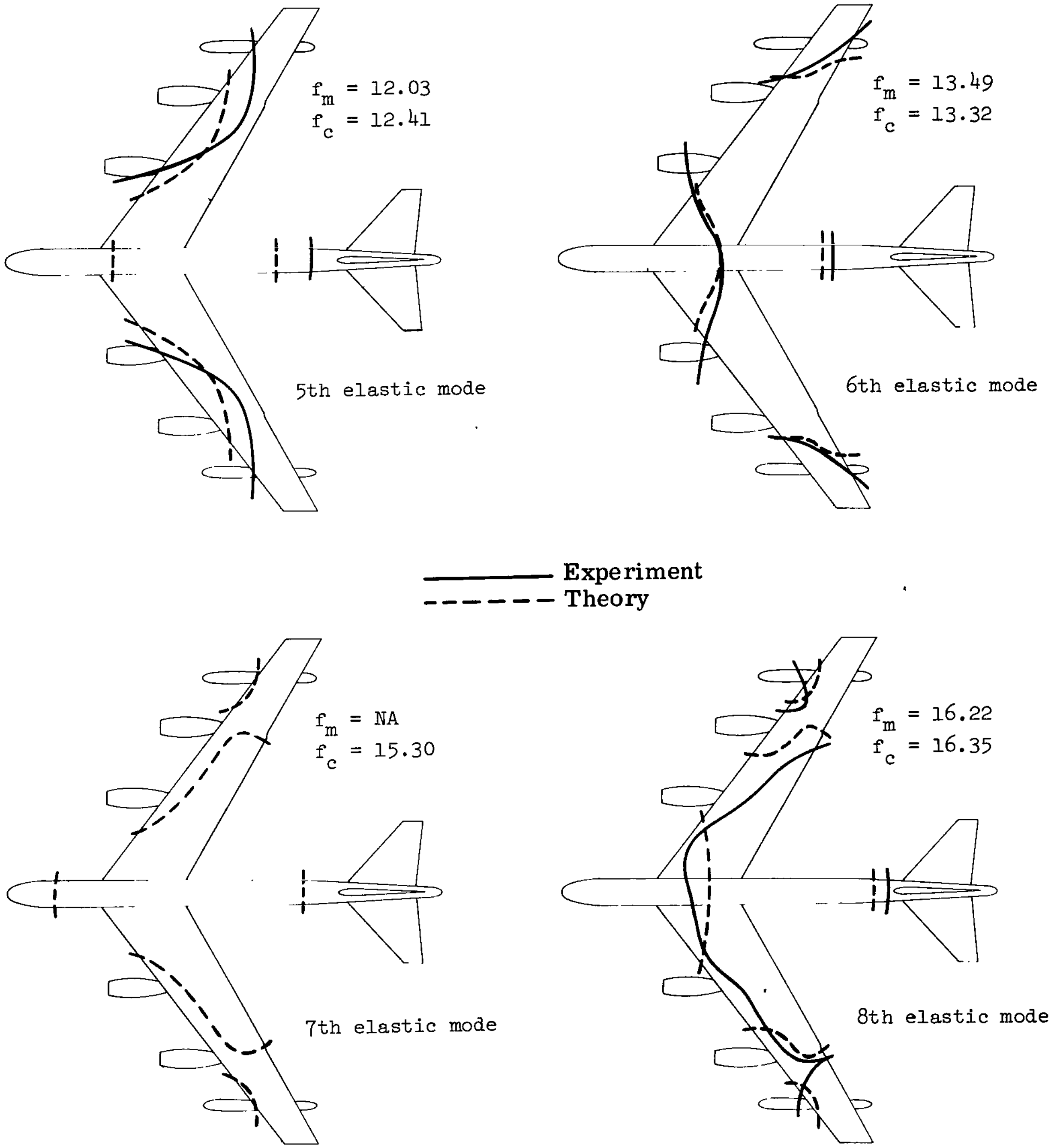

Figure 15.- Concluded.

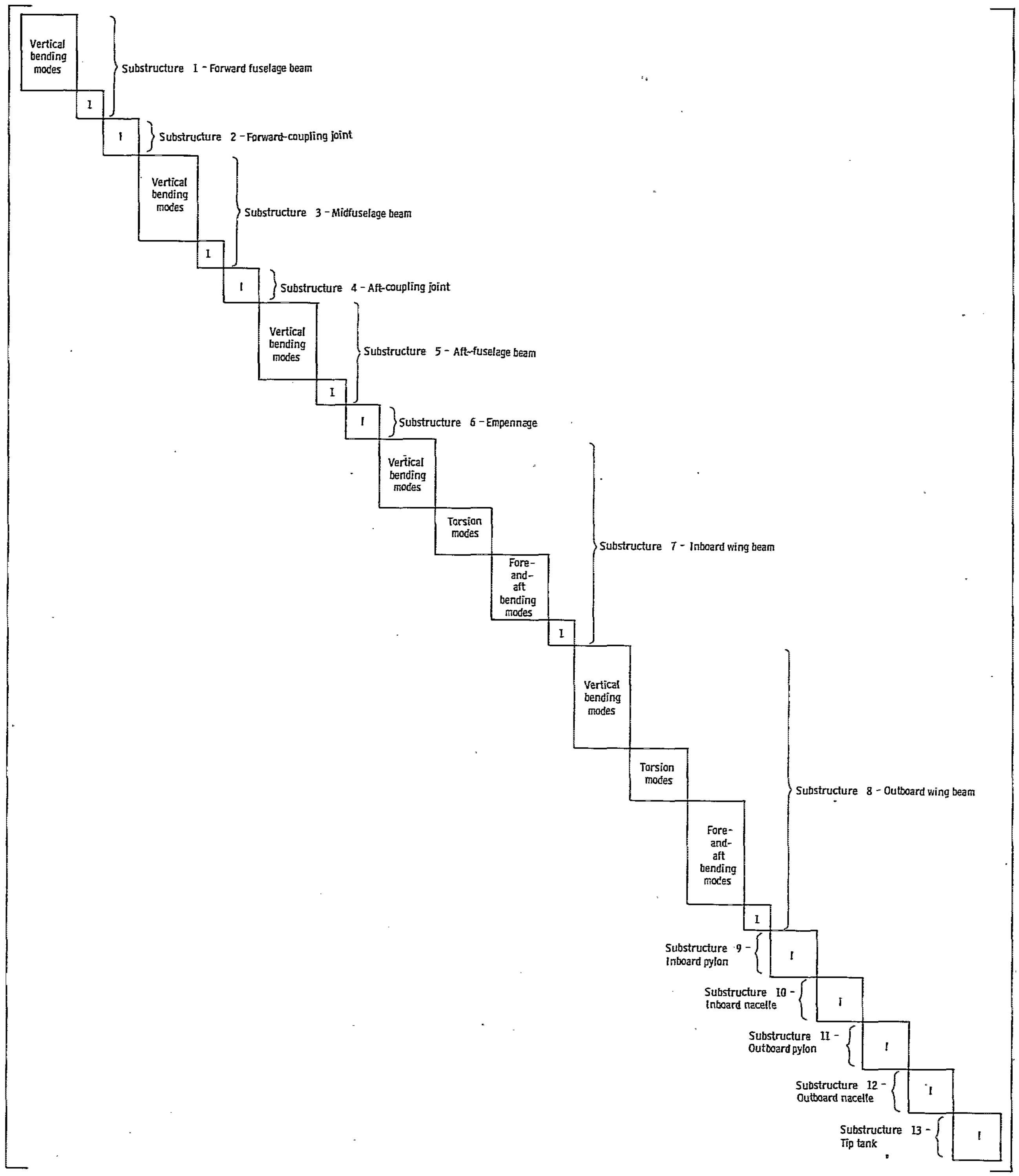

Figure 16.- Block diagonal composition of uncoupled system modal expansion matrix [U] corresponding to the beam representation of the 1/30-scale model of the B-52E airplane given in figure 13.

NATIONAL AERONAUTICS AND SPACE ADMINISTRATION
WASHINGTON, D.C. 20546

OFFICIAL BUSINESS
PENALTY FOR PRIVATE USE $300

SPECIAL FOURTH-CLASS RATE
BOOK

POSTAGE AND FEES PAID
NATIONAL AERONAUTICS AND
SPACE ADMINISTRATION
451

U.S.MAIL

982 001 C1 U D 751010 S00903DS
DEPT OF THE AIR FORCE
AF WEAPONS LABORATORY
ATTN: TECHNICAL LIBRARY (SUL)
KIRTLAND AFB NM 87117

POSTMASTER : If Undeliverable (Section 158 Postal Manual) Do Not Return

"The aeronautical and space activities of the United States shall be conducted so as to contribute . . . to the expansion of human knowledge of phenomena in the atmosphere and space. The Administration shall provide for the widest practicable and appropriate dissemination of information concerning its activities and the results thereof."

—NATIONAL AERONAUTICS AND SPACE ACT OF 1958

NASA SCIENTIFIC AND TECHNICAL PUBLICATIONS

TECHNICAL REPORTS: Scientific and technical information considered important, complete, and a lasting contribution to existing knowledge.

TECHNICAL NOTES: Information less broad in scope but nevertheless of importance as a contribution to existing knowledge.

TECHNICAL MEMORANDUMS: Information receiving limited distribution because of preliminary data, security classification, or other reasons. Also includes conference proceedings with either limited or unlimited distribution.

CONTRACTOR REPORTS: Scientific and technical information generated under a NASA contract or grant and considered an important contribution to existing knowledge.

TECHNICAL TRANSLATIONS: Information published in a foreign language considered to merit NASA distribution in English.

SPECIAL PUBLICATIONS: Information derived from or of value to NASA activities. Publications include final reports of major projects, monographs, data compilations, handbooks, sourcebooks, and special bibliographies.

TECHNOLOGY UTILIZATION PUBLICATIONS: Information on technology used by NASA that may be of particular interest in commercial and other non-aerospace applications. Publications include Tech Briefs, Technology Utilization Reports and Technology Surveys.

Details on the availability of these publications may be obtained from:

SCIENTIFIC AND TECHNICAL INFORMATION OFFICE

NATIONAL AERONAUTICS AND SPACE ADMINISTRATION

Washington, D.C. 20546